DOI: 10.1534/genetics.110.125419

Genetic Analysis Implicates the Set3/Hos2 Histone Deacetylase in the Deposition and Remodeling of Nucleosomes Containing H2A.Z

Mingda Hang* and M. Mitchell Smith*,†,[1]

*Department of Microbiology, University of Virginia Health System, Charlottesville, Virginia 22908 and †University of Virginia Cancer Center, University of Virginia Health System, Charlottesville, Virginia 22908

Manuscript received November 23, 2010
Accepted for publication January 26, 2011

ABSTRACT

Histone variants and histone modification complexes act to regulate the functions of chromatin. In *Saccharomyces cerevisiae* the histone variant H2A.Z is encoded by *HTZ1*. Htz1 is dispensable for viability in budding yeast, but *htz1*Δ is synthetic sick or lethal with the null alleles of about 200 nonessential genes. One of the strongest of these interactions is with the deletion of *SET3*, which encodes a subunit of the Set3/Hos2 histone deacetylase complex. Little is known about the functions of Set3, and interpreting these genetic interactions remains a highly challenging task. Here we report the results of a forward genetic screen to identify bypass suppressors of the synthetic slow-growth phenotype of *htz1*Δ *set3*Δ. Among the identified loss-of-function suppressors are genes encoding subunits of the HDA1 deacetylase complex, the SWR1 complex, the H2B deubiquitination module of SAGA, the proteasome, Set1, and Sir3. This constellation of suppressor genes is uncommon among the global set of *htz1*Δ synthetic interactions. *BDF1*, *AHC1*, *RMR1*, and *CYC8* were identified as high-copy suppressors. We also identified interactions with *SLX5* and *SLX8*, encoding the sumoylation-targeted ubiquitin ligase complex. In the context of *htz1*Δ *set3*Δ, suppressors in the SWR1 and the H2B deubiquitination complexes show strong functional similarity, as do suppressors in the silencing genes and the proteasome. Surprisingly, while both *htz1*Δ *set3*Δ and *swr1*Δ *set3*Δ have severe slow-growth phenotypes, the *htz1*Δ *swr1*Δ *set3*Δ triple mutant grows relatively well. We propose that Set3 has previously unrecognized functions in the dynamic deposition and remodeling of nucleosomes containing H2A.Z.

HIGHLY sophisticated coordination of distinct sets of chromatin regulators is required for the information to flow correctly from DNA to RNA in eukaryotic cells. Reconstructing the temporal and spatial structure of this coordination is the central task of studying eukaryotic gene expression. The direct entry points are physical interactions among the chromatin regulators but many functional relationships are beyond immediate physical interactions and only visible through genetic interactions. Interpreting the genetic interactions in the context of physical process remains extremely challenging. In recent years, functional genomics studies utilizing yeast deletion collection (Tong *et al.* 2001; Ooi *et al.* 2003; Pan *et al.* 2006; Collins *et al.* 2007; Lin *et al.* 2008; Fiedler *et al.* 2009; Costanzo *et al.* 2010) have generated large data sets of genetic interactions but most of these await prioritization and investigation. In this report, we chose to study the genetic interactions between the gene for histone H2A variant *HTZ1* and the gene for *SET3* because of the critical roles of their functional homologs in metazoan development.

The results of early chromatin immunoprecipitation experiments in the budding yeast *Saccharomyces cerevisiae* showed that Htz1 preferentially occupies the promoter regions of two transcriptionally inactive but inducible genes, *GAL1* and *PHO5* (Santisteban *et al.* 2000). This promoter enrichment was later revealed to be a global pattern in budding yeast by several independent studies (Guillemette *et al.* 2005; Li *et al.* 2005; Raisner *et al.* 2005; Zhang *et al.* 2005; Albert *et al.* 2007). Both the protein sequence of H2A.Z and its distinct genomic geography are highly conserved from budding yeast to mammalian cells as the promoter enrichment pattern of H2A.Z has been reported in worm (Whittle *et al.* 2008), fly (Mavrich *et al.* 2008), plant (Zilberman *et al.* 2008), murine (Creyghton *et al.* 2008), and human cells (Barski *et al.* 2007). It is well established in yeast that the ATP-dependent SWR1 complex deposits H2A.Z onto chromatin (Krogan *et al.* 2003; Kobor *et al.* 2004; Mizuguchi *et al.* 2004). Although the specific targeting mechanism remains to be determined, NuA4-mediated histone acetylation and the double bromodomain subunit of SWR1 complex, Bdf1, have been suggested to be the contributing factors of the selective deposition

Supporting information is available online at http://www.genetics.org/cgi/content/full/genetics.110.125419/DC1.

[1]*Corresponding author:* Department of Microbiology, University of Virginia Health System, 1300 Jefferson Park Ave., Box 800734, Charlottesville, VA 22908-0734. E-mail: mms7r@virginia.edu

(Altaf *et al.* 2010). In budding yeast, the Htz1 molecules are removed from the promoters during the activation process of inducible genes (Santisteban *et al.* 2000), which may be partially facilitated by the intrinsic fragility of Htz1–H2B dimer compared to the canonical H2A–H2B dimer (Zhang *et al.* 2005). The detailed mechanism and the relationships between this dynamic process and other transcriptional initiation events are largely unclear. The 5′-end enrichment pattern of H2A.Z appears to be dynamic in metazoan cells as well, observed most prominently during development (Creyghton *et al.* 2008; Whittle *et al.* 2008; Cui *et al.* 2009) and regulated gene expression responding to environmental signals (John *et al.* 2008; Sutcliffe *et al.* 2009). One striking example is in murine embryonic stem cells. H2A.Z molecules occupy the promoters of genes critical for development and this genomic distribution shows remarkable correlations with the patterns of Polycomb group (PcG) proteins. In lineage-committed cells, H2A.Z molecules redistribute to the promoters of different sets of genes (Creyghton *et al.* 2008). The link between H2A.Z and PcG group proteins was revealed earlier by genetic studies in Drosophila (Swaminathan *et al.* 2005). It was reported that the developmental abnormalities of Pc mutants could be enhanced by additional mutation in *His2AV,* the H2A.Z gene in Drosophila. Consistently, the mutant phenotypes of Trithorax group (TrxG) genes, encoding the development regulators antagonizing PcG proteins, could be suppressed by *His2AV* mutation.

In budding yeast, Set3 was found by TAP-tag affinity purification to be a component of a 7-subunit HDAC complex (Pijnappel *et al.* 2001). Based on the complex composition, Set3 complex was proposed to be a functional homolog of metazoan NCoR/SMRT complexes, which are transcriptional corepressors directly interacting with unliganded nuclear receptors to shape the chronology of gene expression through mediating active repression. They play critical roles during development, tissue differentiation and metabolism (Mckenna and O'malley 2002). As a platform, NCoR/SMRT forms various complexes with different sets of subunits to achieve cell-type and promoter specificities. NCoR/SMRT forms a stable ternary complex with histone deacetylase HDAC3 (Guenther *et al.* 2000; Li *et al.* 2000) and TBL1 (Guenther *et al.* 2000), a WD-repeat-containing protein. HDAC3 and TBL1 are mammalian homologs of Hos2 and Sif1, both of which are core subunits of the budding yeast Set3 complex. The functional homology between Set3 complex and NCoR/SMRT extends further to the SANT domain shared by NCoR/SMRT and another core subunit of Set3 complex, Snt1 (Yu *et al.* 2003). Histone methyltransferase activity has not been associated with NCoR/SMRT and no methyltransferase activity has been reported for Set3 complex either. The main enzymatic activity of Set3 complex appears to be the HDAC subunit Hos2, which deacetylates histone H3 and H4 at the 5′ ends of actively transcribing genes. The recruitment of the Set3 complex to the 5′ end requires both the H3K4 methylation and the plant homeo domain of Set3 (Kim and Buratowski 2009). Interestingly, in addition to the different compositions of the NCoR/SMRT complex, another level of specificity of nuclear receptor responses can be achieved by cell-specific localization of H2A.Z. It is reported that H2A.Z plays a critical role in shaping the chromatin signature at the nuclear receptor interaction sites (John *et al.* 2008).

Although it is dispensable for budding yeast to grow under optimal conditions, *htz1*Δ is synthetic sick or lethal with null alleles of about 200 genes, together covering a wide spectrum of cellular functions. A major subgroup of genes having genetic interactions with *htz1*Δ consists of chromatin regulators, among which are the genes encoding the four core subunits of Set3 complex, *SET3*, *HOS2*, *SIF2,* and *SNT1*. The synthetic interaction between Htz1 and Set3 complex suggests overlapping roles in at least one essential biological process. While Htz1 is convincingly involved in a variety of cellular functions such as transcription (Santisteban *et al.* 2000), chromatin boundary maintenance (Meneghini *et al.* 2003), chromosome segregation (Rangasamy *et al.* 2004), and cell-cycle control (Dhillon *et al.* 2006), the function of Set3 complex is relatively poorly examined. Disruption of Set3 complex results in early induction of meiotic gene program upon nitrogen starvation (Pijnappel *et al.* 2001), indicating a repressive role of Set3 complex in transcription, which is reminiscent of its metazoan corepressor homologs. This notion is complicated by another report (Wang *et al.* 2002), which showed that Set3 and Hos2 are required for efficient transcription of *GAL1,* and *HOS2* physically associates with actively transcribing genes. This result has been recently reinforced and the mechanism behind this active role is linked to H3K4 methylation-dependent recruitment of Set3 complex to the 5′ of the gene and Hos2-dependent deacetylation of the region (Kim and Buratowski 2009). The association of Set3 with actively transcribed genes can also be methylation independent, as phosporylation of the Pol II C-terminal domain by Kin28 has been found to stimulate the cotranscriptional recruitment of the Set3 complex to coding regions (Govind *et al.* 2010).

The intricate involvements of both H2A.Z and NCoR/SMRT in some of the most critical biological processes invoked us to gain further insight into their relationship. We propose that the fundamental biology is conserved in the synthetic interaction between their nonessential functional homologs in budding yeast, and we can expand this genetic interaction through yeast genetics, which is of great advantage in this case since the essential requirements of H2A.Z and NCoR/SMRT in higher eukaryotes preclude the task in metazoan system.

MATERIALS AND METHODS

Yeast strains, plasmids, and methods: Yeast strains used in this study are listed in Table 1. Plasmids used are listed in Table 2. Standard yeast manipulations were performed as described (Adams *et al.* 1998). 5-Fluoroortic acid (5-FOA) was added to the final concentration of 1 mg/ml. The concentrations of other drugs are described in relevant contexts. Yeast transformation is based on the lithium acetate method. Cells were grown to 2×10^7 cells/ml, and the transformation mix was subject to heat shock at 42° for 30 min. For recovery of plasmids, 5 ml overnight yeast cultures were resuspended in STET buffer (8% sucrose, 50 mm Tris HCl pH 8.0, 50 mm EDTA, 5% Triton X-100) and mechanically disrupted in the presence of glass beads. After removing the impurities, DNA was ethanol precipitated, recovered, and used to transform a *leu Escherichia coli* strain JA221.

Mutagenesis, screening, and cloning: The *mTn-LEU2/lacZ* yeast genomic library was constructed and described by MacDonald *et al.* (1999). Plasmid DNA collected with midi-prep kit (Qiagen) from the 14 pools of the mTn3 library was digested with *Not*I and gel purified. MSY4477 was transformed with purified DNA and the cells were plated onto SC–Leu plates at about 1200 colonies/large petri dish (150 × 15 mm). Approximately 90,000 colonies were subjected to the subsequent screening. The transformants were microscopically examined and colonies that displayed sectoring phenotype were streaked onto SC–Ura–Leu plates to select the pMSS59[*HTZ1 URA3 ADE3*] plasmids. Nonsectoring red colonies of these candidates from SC–Ura–Leu plates were restreaked onto YPD plates to confirm their sectoring phenotype. Candidates maintaining the sectoring phenotype were crossed with MSY4478, which is isogenic to MSY4477 except for having the opposite mating type. The diploids were subjected to tetrad analysis. If a single transposon-disrupted ORF is responsible for the sectoring phenotype, the sectoring phenotype cosegregates with the *LEU2* marker on the transposon and follow a 2:2 segregation pattern. The transposon insertion sites in the final candidates were determined by inverse PCR. Genomic DNA from these candidates was purified and digested with *Rsa*I. The digested genomic DNA was treated with T4 ligase at low concentration (1 μg/ml) to promote self-ligation. The ligation products were used as PCR templates and amplified using the primer pair 5′-TAAGT TGGGTAACGCCAGGGTTTTC-3′ and 5′-TGTTGCCACTCG CTTTAATG-3′. The PCR products were gel purified and sequenced with primer 5′-CGTTGTAAAACGACGGGATCC CCC-3′. The sequencing results were subject to BLAST search and the transposon insertion sites on the chromosome were determined.

EMS mutagenesis: After the determination of the ethyl methanesulfonate (EMS) kill curve, the actual mutagenesis screen was performed by adding 23 μl EMS (Sigma) to 3 ml fresh cell culture (grown to log phase at 1×10^7 cells/ml). After 1 hr incubation at 28°, 1 ml 5% sodium thiosulfate was added to quench the mutagen. The cell mix was sonicated and diluted, after which 6000 cells were plated onto each YPD plate (150 × 15 mm) to achieve roughly 2000 surviving colonies per plate. Approximately 60,000 cells were subjected to the visual screening as described in the transposon mutagenesis method and 14 suppressor candidates were isolated. These candidates were crossed to MSY4478 to determine whether the suppressor mutations were recessive or dominant, and the resultant diploids were subjected to tetrad analysis. To clone the recessive suppressor candidate, a p366-based yeast genomic library was used to transform the suppressor strain. The Leu^+ transformants were visually screened for revertants displaying nonsectoring color pattern due to the complementation of the suppressor gene by the wild-type copy on the library plasmid.

Generating deletion mutations: All deletion mutants were generated by one-step replacement by homologous recombination. The knockout DNA fragments consisted of the ORF-flanking sequences PCR amplified together with a drug-resistant gene using GoTaq polymerase (Promega). The *natMX* template was plasimd pAG25 and the *hphMX* template was plasmid pAG32 using primers with following features: from 5′ to 3′, forward (reverse) primers have ~40 nucleotides homologous to the 5′ ends (3′ ends) of the genomic target loci followed by 5′-CGTACGCTGCAGGTC GAC-3′ (5′-ATCGATGAATTCGAGCTCG-3′). The PCR products were gel purified (Qiagen) and 1 μg DNA was used for each transformation. After heat shock, cells were recovered in YPD media for at least 4 hr before being plated onto YPD + drug plates (kanamycin, 400 μg/ml; clonNAT, 100 μg/ml; hygromycin B, 500 μg/ml). The transformants were screened by analytical PCR using a forward primer located upstream of the replacement DNA and a common reverse primer located inside the drug-resistant cassette (5′-GTATGGGCTAAATGTACGGGC-3′).

Highcopy suppressor screen: The 1588 clones of the systematic yeast genomic library (Jones *et al.* 2008) were individually cultured overnight at 37° in 200 μl/well LB + kanamycin (50 μg/ml) in 96-well plates. The overnight cultures from all the wells were pooled and plasmids were extracted by midi-prep kit (Qiagen). MSY4477 was transformed with the library plasmids and plated onto SC–Leu in large petri plates. About 40,000 Leu^+ transformants were visually screened for color-sectoring phenotype. The suppressor candidates that showed color sectoring were restreaked onto SC–Ura–Leu plates to select for the pMSS59[*HTZ1 URA3 ADE3]* plasmids and the solid red colony morphology. After this step, the candidates were restreaked again on SC–Leu plates to determine which candidates would maintain the color-sectoring phenotype. The plasmids were extracted from the yeast cells and sequenced to identify the library plasmid and the genes it carried. All individual genes with their endogenous promoters on the candidate library plasmids were subcloned into pRS425, used to transform MSY4477, and tested for their suppressor activities on the basis of color sectoring and 5-FOA sensitivity.

Synthetic genetic array analysis: Yeast strains for the specialized miniarrays were manually selected from the systematic gene knockout collection created in the *MAT***a** BY4741 background (Giaever *et al.* 2002) (EUROSCARF, Institute for Molecular Biosciences, Frankfurt, Germany). Deletions having negative genetic interactions with *htz1*Δ and *set3*Δ were chosen on the basis of annotations in the Saccharomyces Genome Database (http://www.yeastgenome.org). Spreadsheets of the miniarrays are presented in supporting information, Table S1 and Table S2. The query strains were constructed in the background of *MAT*α *can1::Prom-STE2-Sphis5 lyp1*Δ *cyh2 his3*Δ*1 leu2*Δ*0 ura3*Δ*0 met15*Δ*0* (Tong *et al.* 2004). The *htz1*Δ and *set3*Δ alleles were replaced by *natMX* in the single query strains. These two strains were then used to construct the double-query strains, each of which has a suppressor allele replaced by *hphMX*. Synthetic genetic array analysis was carried out as described previously (Tong *et al.* 2004) with the modification including hygromycin, in addition to kanamycin and clonNAT, for the final triple-mutant selection. After 4 days of selection, the growth of the pinned colonies was recorded by digital photography and colony sizes were determined using custom image analysis software based on the Python Imaging Library (Pythonware, http://www.pythonware.com/products/pil/). Colony sizes were normalized across different plates using the set of control strains arrayed with the test sets. Synthetic negative genetic inter-

TABLE 1

Yeast strains

Strains	Genotypes
MSY2029	*MAT***a** *his3Δ1 leu2Δ0 met15Δ0 ura3Δ0*
MSY4477	*MAT***a** *ade2-1 ade3::hisG can1-100 his3-11,15 leu2-3,112 trp1-1 ura3-1 htz1Δ set3Δ::Nat^R pMSS59[HTZ1 URA3 ADE3]*
MSY4478	*MATα ade2-1 ade3::hisG can1-100 his3-11,15 leu2-3,112 trp1-1 ura3-1 htz1Δ set3Δ::Nat^R pMSS59[HTZ1 URA3 ADE3]*
MSY4100	*MATα can1::Prom-STE2-Sphis5 lyp1Δ cyh2 his3Δ1 leu2Δ0 ura3Δ0 met15Δ0 htz1Δ::Nat^R*
MSY4506	*MATα can1::Prom-STE2-Sphis5 lyp1Δ cyh2 his3Δ1 leu2Δ0 ura3Δ0 met15Δ0 htz1Δ::Nat^R swr1Δ::hph^R*
MSY4652	*MATα can1::Prom-STE2-Sphis5 lyp1Δ cyh2 his3Δ1 leu2Δ0 ura3Δ0 met15Δ0 htz1Δ::Nat^R vps72Δ::hph^R*
MSY4653	*MATα can1::Prom-STE2-Sphis5 lyp1Δ cyh2 his3Δ1 leu2Δ0 ura3Δ0 met15Δ0 htz1Δ::Nat^R hda2Δ::hph^R*
MSY4654	*MATα can1::Prom-STE2-Sphis5 lyp1Δ cyh2 his3Δ1 leu2Δ0 ura3Δ0 met15Δ0 htz1Δ::Nat^R hda3Δ::hph^R*
MSY4508	*MATα can1::Prom-STE2-Sphis5 lyp1Δ cyh2 his3Δ1 leu2Δ0 ura3Δ0 met15Δ0 htz1Δ::Nat^R ubp8Δ::hph^R*
MSY4655	*MATα can1::Prom-STE2-Sphis5 lyp1Δ cyh2 his3Δ1 leu2Δ0 ura3Δ0 met15Δ0 htz1Δ::Nat^R sgf11Δ::hph^R*
MSY4509	*MATα can1::Prom-STE2-Sphis5 lyp1Δ cyh2 his3Δ1 leu2Δ0 ura3Δ0 met15Δ0 htz1Δ::Nat^R rpn10Δ::hph^R*
MSY4656	*MATα can1::Prom-STE2-Sphis5 lyp1Δ cyh2 his3Δ1 leu2Δ0 ura3Δ0 met15Δ0 htz1Δ::Nat^R pre9Δ::hph^R*
MSY4537	*MATα can1::Prom-STE2-Sphis5 lyp1Δ cyh2 his3Δ1 leu2Δ0 ura3Δ0 met15Δ0 set3Δ::Nat^R*
MSY4657	*MATα can1::Prom-STE2-Sphis5 lyp1Δ cyh2 his3Δ1 leu2Δ0 ura3Δ0 met15Δ0 set3Δ::Nat^R hda2Δ::hph^R*
MSY4658	*MATα can1::Prom-STE2-Sphis5 lyp1Δ cyh2 his3Δ1 leu2Δ0 ura3Δ0 met15Δ0 set3Δ::Nat^R hda3Δ::hph^R*
MSY4659	*MATα can1::Prom-STE2-Sphis5 lyp1Δ cyh2 his3Δ1 leu2Δ0 ura3Δ0 met15Δ0 set3Δ::Nat^R ubp8Δ::hph^R*
MSY4660	*MATα can1::Prom-STE2-Sphis5 lyp1Δ cyh2 his3Δ1 leu2Δ0 ura3Δ0 met15Δ0 set3Δ::Nat^R sgf11Δ::hph^R*
MSY4661	*MATα can1::Prom-STE2-Sphis5 lyp1Δ cyh2 his3Δ1 leu2Δ0 ura3Δ0 met15Δ0 set3Δ::Nat^R rpn10Δ::hph^R*
MSY4662	*MATα can1::Prom-STE2-Sphis5 lyp1Δ cyh2 his3Δ1 leu2Δ0 ura3Δ0 met15Δ0 set3Δ::Nat^R pre9Δ::hph^R*
MSY4586	*MAT***a** *his3Δ1 leu2Δ0 met15Δ0 ura3Δ0 htz1Δ::Nat^R*
MSY4587	*MAT***a** *his3Δ1 leu2Δ0 met15Δ0 ura3Δ0 htz1Δ::Nat^R hda1Δ::hph^R*
MSY4588	*MAT***a** *his3Δ1 leu2Δ0 met15Δ0 ura3Δ0 htz1Δ::Nat^R hda2Δ::hph^R*
MSY4589	*MAT***a** *his3Δ1 leu2Δ0 met15Δ0 ura3Δ0 htz1Δ::Nat^R swr1Δ::hph^R*
MSY4590	*MAT***a** *his3Δ1 leu2Δ0 met15Δ0 ura3Δ0 htz1Δ::Nat^R arp6Δ::hph^R*
MSY4591	*MAT***a** *his3Δ1 leu2Δ0 met15Δ0 ura3Δ0 htz1Δ::Nat^R ubp8Δ::hph^R*
MSY4592	*MAT***a** *his3Δ1 leu2Δ0 met15Δ0 ura3Δ0 htz1Δ::Nat^R sgf11Δ::hph^R*
MSY4593	*MAT***a** *his3Δ1 leu2Δ0 met15Δ0 ura3Δ0 htz1Δ::Nat^R set1Δ::hph^R*
MSY4594	*MAT***a** *his3Δ1 leu2Δ0 met15Δ0 ura3Δ0 htz1Δ::Nat^R sir3Δ::hph^R*
MSY4595	*MAT***a** *his3Δ1 leu2Δ0 met15Δ0 ura3Δ0 htz1Δ::Nat^R rpn9Δ::hph^R*
MSY4596	*MAT***a** *his3Δ1 leu2Δ0 met15Δ0 ura3Δ0 htz1Δ::Nat^R rpn10Δ::hph^R*
MSY4544	*MAT***a** *ade2-1 ade3::hisG can1-100 his3-11,15 leu2-3,112 trp1-1 ura3-1 htz1Δ set3Δ::Nat^R pMSS59[HTZ1 URA3 ADE3] pMH02 [SLX5 TRP1 CEN]*
MSY4605	*MAT***a** *his3Δ1 leu2Δ0 met15Δ0 ura3Δ0 htz1Δ::Nat^R* pRS425
MSY4606	*MAT***a** *his3Δ1 leu2Δ0 met15Δ0 ura3Δ0 htz1Δ::Nat^R* pMH05[*AHC1 LEU2* 2μ]
MSY4607	*MAT***a** *his3Δ1 leu2Δ0 met15Δ0 ura3Δ0 htz1Δ::Nat^R* pMH04[*BDF1 LEU2* 2μ]
MSY4608	*MAT***a** *his3Δ1 leu2Δ0 met15Δ0 ura3Δ0 htz1Δ::Nat^R* pMH07[*CYC8 LEU2* 2μ]
MSY4609	*MAT***a** *his3Δ1 leu2Δ0 met15Δ0 ura3Δ0 htz1Δ::Nat^R* pMH06[*RMR1 LEU2* 2μ]
MSY4603	*MAT***a** *his3Δ1 leu2Δ0 met15Δ0 ura3Δ0 set3Δ::Kan^R*
MSY4610	*MAT***a** *his3Δ1 leu2Δ0 met15Δ0 ura3Δ0 set3Δ::Kan^R hda1Δ::hph^R*
MSY4611	*MAT***a** *his3Δ1 leu2Δ0 met15Δ0 ura3Δ0 set3Δ::Kan^R hda2Δ::hph^R*
MSY4612	*MAT***a** *his3Δ1 leu2Δ0 met15Δ0 ura3Δ0 set3Δ::Kan^R ubp8Δ::hph^R*
MSY4613	*MAT***a** *his3Δ1 leu2Δ0 met15Δ0 ura3Δ0 set3Δ::Kan^R sgf11Δ::hph^R*
MSY4614	*MAT***a** *his3Δ1 leu2Δ0 met15Δ0 ura3Δ0 set3Δ::Kan^R set1Δ::hph^R*
MSY4615	*MAT***a** *his3Δ1 leu2Δ0 met15Δ0 ura3Δ0 set3Δ::Kan^R sir3Δ::hph^R*
MSY4616	*MAT***a** *his3Δ1 leu2Δ0 met15Δ0 ura3Δ0 set3Δ::Kan^R rpn10Δ::hph^R*
MSY4617	*MAT***a** *his3Δ1 leu2Δ0 met15Δ0 ura3Δ0 set3Δ::Kan^R* pRS425
MSY4618	*MAT***a** *his3Δ1 leu2Δ0 met15Δ0 ura3Δ0 set3Δ::Kan^R* pMH05[*AHC1 LEU2* 2μ]
MSY4619	*MAT***a** *his3Δ1 leu2Δ0 met15Δ0 ura3Δ0 set3Δ::Kan^R* pMH04[*BDF1 LEU2* 2μ]
MSY4620	*MAT***a** *his3Δ1 leu2Δ0 met15Δ0 ura3Δ0 set3Δ::Kan^R* pMH07[*CYC8 LEU2* 2μ]
MSY4621	*MAT***a** *his3Δ1 leu2Δ0 met15Δ0 ura3Δ0 set3Δ::Kan^R* pMH06[*RMR1 LEU2* 2μ]
MSY4523	*MAT***a***URA3-TEL-VIIL ppr1::TRP1 ura3Δ0 trp1-Δ63* (1)
MSY4528	*MAT***a***URA3-TEL-VIIL ppr1::TRP1 ura3Δ0 trp1-Δ63 sir3Δ::hph^R*
MSY4529	*MAT***a***URA3-TEL-VIIL ppr1::TRP1 ura3Δ0 trp1-Δ63 rpn10Δ::hph^R*
MSY4531	*MAT***a***URA3-TEL-VIIL ppr1::TRP1 ura3Δ0 trp1-Δ63 ubp14Δ::hph^R*
MSY4663	*MAT***a** *ade2-1 can1-100 his3-Δ200 leu2-3,112 trp1 URA3::TelVR* (2)
MSY4664	*MAT***a** *ade2-1 can1-100 his3-Δ200 leu2-3,112 trp1 URA3::TelVR sir3Δ::hph^R*
MSY4665	*MAT***a** *ade2-1 can1-100 his3-Δ200 leu2-3,112 trp1 URA3::TelVR rpn10Δ::hph^R*
MSY4666	*MAT***a** *ade2-1 can1-100 his3-Δ200 leu2-3,112 trp1 URA3::TelVR ubp14Δ::hph^R*
MSY4667	*MAT***a** *ade2-1 can1-100 his3-Δ200 leu2-3,112 trp1 URA3::TelVR hda1Δ::hph^R*

All strains were constructed during this study except for: (1) Kahana and Gottschling (1999) and (2) Rundlett *et al.* (1996).

actions were scored using as a cutoff a reduction of at least 25% in colony spot size relative to the single mutant alone. Bypass suppression was scored using a criterion of an increase in colony spot size of at least 33% with the suppressor relative to the double-mutant strain. For *htz1*Δ, each interacting deletion strain was represented once on the array (Table S1) and each candidate suppressor was screened in three independent experiments. For *set3*Δ, each deletion strain was represented three times on the array (Table S2) and each suppressor was screened once.

RESULTS

Isolation of *htz1*Δ *set3*Δ bypass suppressor mutations: To characterize the network of *HTZ1* and *SET3* genetic interactions, we sought to isolate suppressors of the *htz1*Δ *set3*Δ slow-growth phenotype using a colony color screen (Bender and Pringle 1991). Growth of the *htz1*Δ *set3*Δ strain MSY4477 is maintained by the presence of plasmid pMSS59[*HTZ1 URA3 ADE3*], which also confers 5-FOA sensitivity and nonsectoring red colony color. The introduction of a suppressor mutation that bypasses the *htz1*Δ *set3*Δ synthetic slow-growth phenotype allows the plasmid to be lost during mitotic growth, giving rise to red/white sectored colonies and the segregation of 5-FOA-resistant isolates. We exploited the sectoring pattern for visual screening and 5-FOA resistance for secondary characterization.

Bypass suppressors were generated by transposon mutagenesis (Ross-MacDonald *et al.* 1999). Pooled DNA prepared from the transposon library was used to transform MSY4477 and ~90,000 Leu^+ transformants were subjected to several steps of screening and verification (materials and methods). DNA sequence analysis of the transposon gene disruptions identified the following 12 candidate suppressor genes (and the number of times each was isolated): *hda2* (7), *hda3* (10), *ubp8* (2), *sgf11* (3), *swr1* (2), *vps72* (2), *arp6* (3), *set1* (1), *sir3* (2), *rpn10* (3), *pre9* (2), and *ubp14* (1). These candidates were crossed to MSY4478 and the diploids were subjected to tetrad analysis (*sir3* was not tested due to sterility). In all cases, the sectoring phenotype segregated together with the transposon disrupted allele, marked by *LEU2*, and the tetrads showed 2:2 segregation. Finally, we confirmed the identities of the suppressors by deleting each of the candidate genes in MSY4477 and found that all the deletions resulted in strong suppression of the *htz1*Δ *set3*Δ synthetic slow-growth phenotype (Figure 1, A and B).

One striking feature of this collection is that most of the genes encode subunits of protein complexes with broad functional significance, including the trimeric Hda1 histone deacetylation complex (*hda2*, *hda3*), the H2B deubiquitination submodule of the SAGA complex (*ubp8*, *sgf11*), the SWR1 complex (*swr1*, *arp6*, *vps72*), and the proteasome (*rpn10*, *pre9*). Thus, we next tested whether the deletion of other nonessential subunits of these complexes could also suppress *htz1*Δ *set3*Δ (data not shown). We found that deletions of the genes encoding all three subunits of the Hda1 HDAC complex, including *HDA1,* which encodes the enzymatic subunit, suppress *htz1*Δ *set3*Δ. In the case of the SAGA complex, only deletion of the H2B deubiquitination module genes could suppress. We tested the deletion of three genes outside the H2B deubiquitination module (*gcn5*, *spt3*, and *spt8)* and found that they actually exacerbate the synthetic phenotype of *htz1*Δ *set3*Δ. Deletions of all the nonessential subunits of the SWR1 complex, except *YAF9*, are strong suppressors, and the same is true for all the nonessential subunits of the proteasome. These results collectively indicate that it is the functions of these multisubunit protein complexes that become toxic in the absence of Htz1 and Set3.

***SLX5* is a dosage inhibitor of a subset of suppressors:** We also isolated 13 recessive suppressor mutations following random mutagenesis with EMS. We attempted to clone the corresponding wild-type alleles by complementation using a wild-type yeast genomic plasmid library and screening for restoration of the nonsectoring color colony phenotype. Out of ~60,000 transformants of one candidate strain, we repeatedly isolated two different *CEN* plasmids, both containing *SLX5*. Surprisingly, however, DNA sequence analysis showed that the the candidate suppressor strain did not contain mutations in either the ORF or the promoter region of chromosomal *SLX5*. To confirm this unexpected result, we cloned the chromosomal copy of *SLX5* from the suppressor strain into a *CEN* yeast shuttle vector (pRS315), transformed the candidate suppressor strain with this plasmid, and found that it also restored the nonsectoring phenotype. Thus, while the suppressor mutation in the candidate strain remains unidentified, these results did reveal that an extra gene dose of *SLX5* inhibits suppression. Transformation of *htz1*Δ *set3*Δ double mutants with a *CEN* plasmid copy of wild-type *SLX5* also eliminates the marginal viability of the strain. Interestingly, *SLX8* has a similar, although milder, effect (data not shown).

Slx5 and Slx8 comprise a SUMOylation targeted ubiquitin ligase (STUbL) complex, a functionally conserved entity from fission yeast to human cells. Slx5 binds to the SUMOylated subunit and Slx8 acts as the E3

TABLE 2

Plasmids strains

Plasmid name	Genes on plasmid
pMSS59	*HTZ1 URA3 ADE3* 2μ
pMH02	*SLX5 TRP1 CEN6 ARSH4*
pMH03	*SLX8 TRP1 CEN6 ARSH4*
pMH04	*BDF1 LEU2* 2μ
pMH05	*AHC1 LEU2* 2μ
pMH06	*RMR1 LEU2* 2μ
pMH07	*CYC8 LEU2* 2μ
pMH08	*SLX5 LEU2 CEN6 ARSH4*
pMH10	*SIR3 TRP1* 2μ

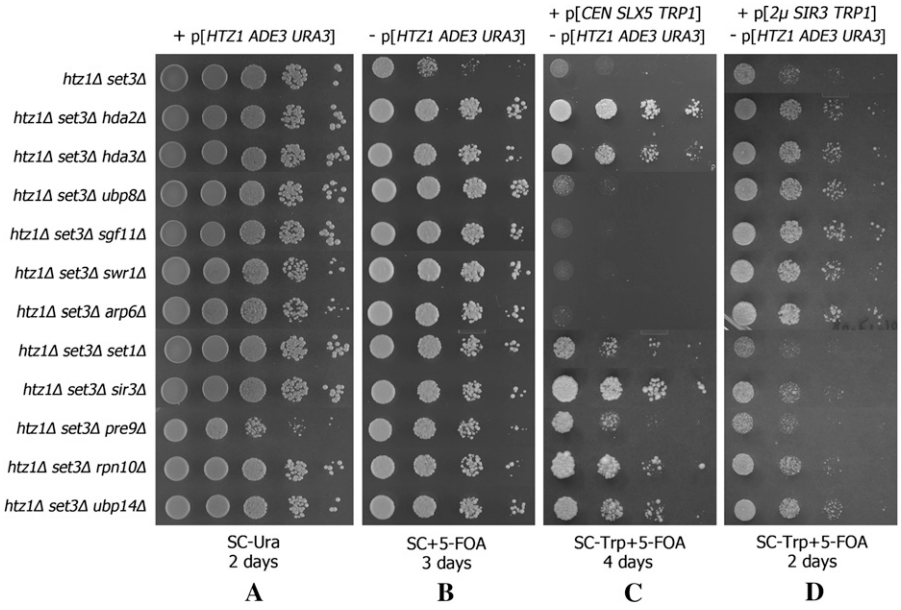

Figure 1.—Loss-of-function suppressors of the *htz1*Δ *set3*Δ synthetic slow-growth phenotype. (A) The indicated strains were cultured in SC–Ura media in the presence of pMSS59[*HTZ1 ADE3 URA3*]. Serial dilutions were plated on SC–Ura plates and grown for 2 days. (B) Small portions of the overnight cell cultures from A were resuspended in YPD and grown overnight to allow the segregational loss of pMSS59. Serial dilutions were plated on SC + 5-FOA plates and grown for 3 days. (C) Differential responses of suppressors to *SLX5* overexpression. The indicated strains were transformed with pMH02[*SLX5 TRP1*] and the transformants were grown overnight in SC–Trp media to permit the loss of pMSS59 while maintaining pMH02. Serial dilutions of the overnight cultures were plated on SC–Trp + 5-FOA plates and grown for 4 days. (D) Differential responses of suppressors to *SIR3* overexpression. The indicated strains were transformed with plasmid pMH10[2μ *SIR3 TRP1*] and the transformants were grown in SC–Trp media overnight to permit the loss of pMSS59 while maintaining pMH10. Serial dilutions of the overnight cultures were plated on SC–Trp + 5-FOA plates and grown for 2 days.

ligase (Burgess *et al.* 2007; Li *et al.* 2007b; Mullen and Brill 2008). This heterodimer complex has been proposed to participate in DNA repair (Zhang *et al.* 2006; Burgess *et al.* 2007; Li *et al.* 2007a; Nagai *et al.* 2008), telomere silencing (Darst *et al.* 2008), and protein quality control (Wang and Prelich 2009). No endogenous SUMOylated substrates of the Slx5–Slx8 complex have been identified although two recent reports identified mating-type switching regulators alpha2 (Xie *et al.* 2010) and alpha1 (Nixon *et al.* 2010) to be un-SUMOylated endogenous substrates.

Phenotypic classification of *htz1*Δ *set3*Δ suppressors: We took advantage of the serendipitous discovery that *SLX5* could eliminate the activity of at least one suppressor and tested the effect of a pMH02[*SLX5 CEN TRP1*] plasmid on our set of known transposon-mediated suppressor mutations. Deletion of genes encoding the SWR1 complex and the H2B deubiquitination module of SAGA complex were no longer able to bypass *htz1*Δ *set3*Δ in the presence of extra copies of *SLX5*. However, the other gene deletions retained the ability to suppress (Figure 1, B and C).

The isolation of *sir3* as a suppressor of *htz1*Δ *set3*Δ indicates that this silent information regulator becomes toxic in the absence of Htz1 and Set3, and the direct removal of this genetic toxin is sufficient to rescue the double mutant. Set1-mediated H3K4 methylation contributes to preventing Sir3 from spreading into euchromatin and *set1*Δ causes dilution of the limited pool of cellular Sir3 from its physiological targets (Venkatasubrahmanyam *et al.* 2007). We hypothesized that the suppressor activity of *set1*Δ might be an indirect consequence of mimicking Sir3 depletion and predicted that its suppressor activity would be reduced by overexpressing *SIR3*. Consistent with this hypothesis, suppression by *set1*Δ was impaired when *SIR3* was overexpressed. Surprisingly, however, the suppression phenotypes exhibited by *rpn10*Δ, *pre9*Δ, and *ubp14*Δ were also notably reduced in the presence of the *SIR3* 2μ plasmid (Figure 1, B and D). Thus, on the basis of their distinct responses to overexpression of either *SLX5* or *SIR3*, the bypass suppressors can be categorized into three phenotypic classes (Table 3).

Telomere silencing requires the protein degradation pathway: The responses of *rpn10*Δ, *pre9*Δ, and *ubp14*Δ to *SIR3* overexpression suggested that the protein degradation pathway might have a previously unrecognized role in Sir3-dependent silencing. To test this, subtelomeric position effect variegation (PEV) was examined in these mutants. PEV was measured by monitoring the 5-FOA sensitivity of a strain in which *URA3* is integrated ~2.1 kb away from the right end of chromosome V (Rundlett *et al.* 1996). *URA3* is randomly silenced in wild-type clonal cells (Figure 2A). Deletion of *SIR3* substantially removes the clonal repression as expected. Interestingly, *ubp14*Δ and *rpn10*Δ both show strong *URA3* derepression at a level comparable to *sir3*Δ (Figure 2A). Deletion of *HDA1*, whose suppression activity does not respond to *SIR3* overexpression, increases subtelomeric silencing, consistent with previous results (Rundlett *et al.* 1996).

To further confirm this novel relationship between *SIR3* and protein degradation, we used another reporter strain in which the *URA3* reporter gene is integrated at the left tip of chromosome VII (Kahana and Gottschling 1999). This strain is barely viable on plates lacking uracil because *URA3* is strictly silenced.

TABLE 3

Categorization of loss of function suppressors into three classes on the basis of their responses to overexpression of *SLX5* or *SIR3*

Suppressors	Suppression in the presence of	
	SLX5(*CEN*)	*SIR3*(2μ)
Hda1 complex	Yes	Yes
SWR1 complex	No	Yes
Ubp8–Sgf11	No	Yes
Set1	Yes	Reduced
Sir3	Yes	Reduced
Proteolytic factors	Yes	Reduced

In this strain *sir3*Δ dramatically improves growth on Ura⁻ plates as expected because of the derepression of *URA3*. Consistent with our PEV results at the telomere of chromosome V, *rpn10*Δ and *ubp14*Δ also increase *URA3* expression (Figure 2B) although the derepression in *rpn10*Δ and *ubp14*Δ is at a lower level compared to *sir3*Δ, as indicated by the growth on 5-FOA plates.

We investigated whether the silencing defects of the protein degradation mutants are associated with a decrease of Sir3 at the telomere region. We introduced *rpn10*Δ and *ubp14*Δ into a strain carrying an allele of *SIR3* encoding a triple-HA epitope tag at the C terminus of Sir3. Sir3–3HA binding at the right end of chromosome V in these deletion mutants was then compared to wild type using chromatin immunoprecipitation (ChIP). No differences between these deletion mutants and the wild-type strain were observed (data not shown), suggesting that in addition to Sir3 binding, one or more additional steps involving the protein degradation pathway are required for efficient telomere silencing.

Suppression of *htz1*Δ and *set3*Δ single defects: The *htz1*Δ *set3*Δ double mutant encounters genetic stress from each of the gene deletions individually as well as the synthetic effect of the double deletion. Thus, in principle, we might expect at least three classes of suppressors: those that bypass one or the other of the single deletions and those that bypass the synthetic defects. Indeed, *hda1*Δ has been reported to rescue the growth phenotype of *htz1*Δ and reduce its sensitivity to hydroxyurea (HU), methyl-methanesulfonate (MMS), and the microtubule-interfering drug benomyl (Lin *et al.* 2008). Therefore, we investigated the effect of the other *htz1*Δ *set3*Δ suppressors on *htz1*Δ single-mutant defects. A series of double mutants containing *htz1*Δ and each of the suppressor genes were constructed in the BY4741 strain background. Their growth conditions on YPD and in the presence of various drugs were compared to wild-type and *htz1*Δ cells. Each functional module was represented by two members to monitor the phenotypic consistency within the group.

In agreement with the observations of Lin *et al.* (2008), disruption of the Hda1 complex weakly suppresses the sensitivities of *htz1*Δ to HU and benomyl and strongly suppresses its MMS sensitivity (Figure 3A). Suppressors within the SWR1 complex genes also improve the growth of *htz1*Δ in the presence of these drugs, but with a more prominent effect on HU sensitivity (Figure 3A). Deletions of genes encoding the SAGA H2B deubiquitination module strongly rescue benomyl sensitivity but only display subtle effects on the sensitivities to the DNA-damaging reagents (Figure 3A). In the case of 6-azauracil (6-AU) and mycophenolic acid (MPA), two drugs that affect transcription elongation by reducing the cellular pool of ribonucleotides, both *swr1*Δ and *ubp8*Δ but not *hda2*Δ, reduce the sensitivity of *htz1*Δ (Figure 3B).

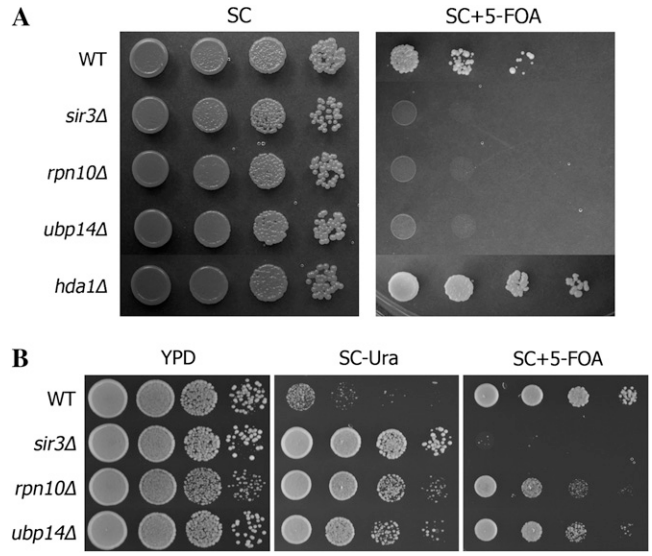

Figure 2.—Sir3-dependent telomere silencing requires the protein degradation pathway. (A) The indicated strains were constructed in a reporter strain in which the *URA3* gene is inserted approximately 2.1 kb away from the left end of the chromosome VII (Rundlett *et al.* 1996). Serial dilutions were plated on SC and SC + 5-FOA plates. (B) The indicated strains were constructed in a reporter strain in which the *URA3* gene is placed at the very end of the chromosome V (kahana and gottschling 1999). Serial dilutions were plated on YPD, SC–Ura, and SC + 5-FOA plates.

We carried out a similar set of tests for *set3*Δ. Fewer phenotypes are known for *set3*; however, the deletion strain is hypersensitive to MPA (Kim and Buratowski 2009) and tunicamycin (Cohen *et al.* 2008), which induces secretory stress response. We again constructed a set of double mutants containing *set3*Δ and each of the suppressor genes and assayed their growth in the presence of MPA and tunicamycin. The *set3*Δ *swr1*Δ and *set3*Δ *arp6*Δ double mutants could not be made due to synthetic lethality between *set3*Δ and loss of SWR1 complex function in the background of BY4741. As expected, MPA markedly inhibited the growth of *set3*Δ. Among the tested suppressors, only those in the H2B deubiquitination module show an ability to rescue the drug sensitivities (Figure 4). Interestingly, *set1*Δ, *sir3*Δ,

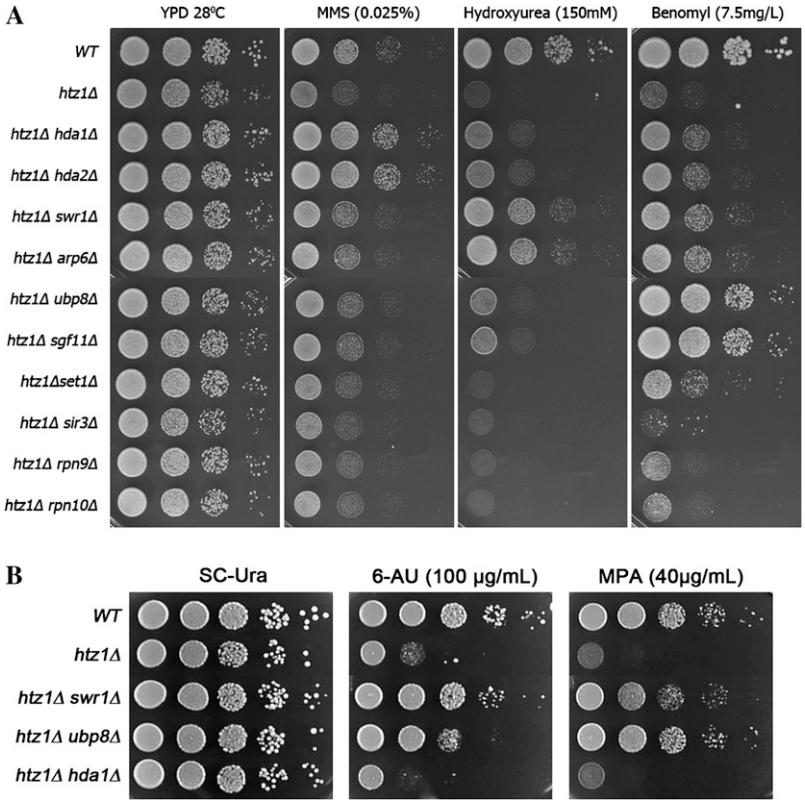

FIGURE 3.—Suppression of *htz1*Δ drug phenotypes by gene deletions. (A) Serial dilutions were plated on YPD, YPD + MMS (0.025%), YPD + hydroxyurea (150 mM), and YPD + benomyl (7.5 μg/ml). (B) The indicated strains were transformed with the control plasmid pRS316 [*URA3 CEN*] and serial dilutions were plated on SC–Ura, SC–Ura + 6-AU (100 μg/ml) and SC–Ura + MPA (40 μg/ml).

and the deletion of genes encoding proteasome subunits all rescue the tunicamycin sensitivity of *set3*Δ cells (Figure 4), providing additional evidence for the functional relationship between Sir3 and the protein degradation pathway.

Bypass suppressors *ubp8*Δ and *sgf11*Δ can act at the level of Htz1- and Set3-dependent gene expression: We next sought to determine if any of the *htz1*Δ *set3*Δ bypass suppressors might be acting at the level of Htz1- and Set3-dependent gene transcription. The hypersensitivity of *htz1*Δ to benomyl is due, in part, to reduced transcription of *RBL2* and *CIN4*, two genes encoding factors required for β-tubulin folding (A. ALLISON, M. SANTISTEBAN, and M.M.S., unpublished results). Since suppressors in genes encoding the Hda1 complex, SWR1 complex, and H2B deubiquitination subcomplex suppress the benomyl sensitivity of *htz1*Δ, we assayed the levels of *RBL2* and *CIN4* mRNAs in these suppressor strains. As expected, the mRNA levels of *RBL2* and *CIN4* in *htz1*Δ are significantly lower than in wild-type cells (Figure 5A). In the case of the tested suppressors, the pattern of mRNA expression matched that of the benomyl sensitivity (Figure 3A). The most potent suppressors of *htz1*Δ benomyl sensitivity are *ubp8* and *sgf11*. Similarly, *CIN4* transcription is markedly increased in *ubp8* and *sgf11* (Figure 5A). Lesser effects are observed for *hda1*Δ, *hda2*Δ, *swr1*Δ, and *arp6*Δ.

The induction of *GAL1* transcription is known to be impaired in *set3*Δ (WANG *et al.* 2002; KIM and BURATOWSKI 2009). Therefore, since *ubp8*Δ and *sgf11*Δ are strong suppressors of the MPA phenotype of *set3*Δ, we compared the induction of *GAL1* transcription in wild type, *set3*Δ, *set3*Δ *ubp8*Δ, and *set3*Δ *sgf11*Δ. Consistent with the previous reports, induction of *GAL1* transcription is notably slower in *set3*Δ cells. Interestingly, *GAL1* transcription is partially restored in *set3*Δ *ubp8*Δ and *set3*Δ *sgf11*Δ (Figure 5B). Together, these results define examples in which bypass suppressors *ubp8*Δ and *sgf11*Δ affect Htz1- and Set3-dependent gene transcription.

Suppression of the global set of *htz1*Δ and *set3*Δ negative genetic interactions: All of the suppressors isolated in our genetic screen are general factors with broad roles in gene expression, rather than regulators of a specific gene or pathway. Consequently, we reasoned that this set of suppressors might be rather general and bypass most synthetic defects involving *htz1*Δ or *set3*Δ. To test this prediction, we carried out a modified synthetic genetic array (SGA) analysis to assess the genome-wide suppression of *htz1*Δ and *set3*Δ negative genetics interactions (Figure 6). First, for each of the *htz1*Δ *set3*Δ bypass suppressor genes, we created a pair of query strains carrying both the suppressor deletion and either *htz1*Δ or *set3*Δ. These double-mutant query strains were then crossed against specialized miniarrays that included strains with gene deletions that have negative genetic interactions with either *htz1*Δ or *set3*Δ (MATERIALS AND METHODS). Control strains that show no genetic interactions with *htz1*Δ and *set3*Δ were also included in the arrays to normalize colonies sizes across replicate plates. After mating with the query

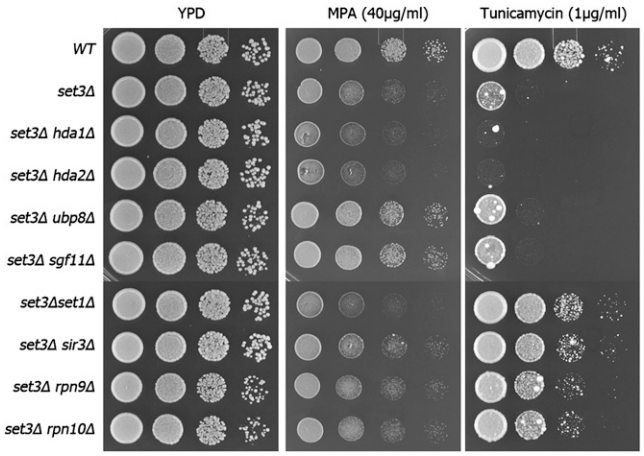

FIGURE 4.—Suppression of *set3*Δ drug phenotypes by gene deletions. Serial dilutions were plated on YPD, YPD + MPA (40 μg/ml), and YPD + tunicamycin (1 μg/ml).

strain and sporulation, the triple mutants were selected and their relative colony sizes were quantified.

The *htz1*Δ-based miniarray was composed of 241 strains with gene deletions known or suspected to produce negative genetic interactions. In control screens where bypass suppressors were not included, 164 gene deletions in the miniarray scored as having negative genetic interactions with *htz1*Δ. We next analyzed the ability of *hda2*Δ, *hda3*Δ, *swr1*Δ, *vps72*Δ, *ubp8*Δ, *sgf11*Δ, *pre9*Δ, and *rpn10*Δ to suppress these negative synthetic genetic interactions. Contrary to expectations, each suppressor only bypassed a limited number of interactions (Table 4 and Table S3). Furthermore, the *htz1*Δ *set3*Δ suppressors, as a group, did not function coordinately to suppress other *htz1*Δ synthetic interactions. Only 14 of the 164 negative genetic interactions were bypassed by at least 7 of the suppressors, and growth of the average double mutant was improved by less than 3 of the *htz1*Δ *set3*Δ suppressors.

The *set3*Δ miniarray was composed of 53 gene deletions. Of these, 25 deletions were scored as having a synthetic negative growth phenotype in combination with *set3*Δ. Since *swr1*Δ and *vps72*Δ are themselves synthetic lethal with *set3*Δ in the SGA strain background, we could create only double-mutant query strains with *hda2*Δ, *hda3*Δ, *ubp8*Δ, *sgf11*Δ, *pre9*Δ, and *rpn10*Δ. As with the *htz1*Δ analysis, most of the 25 synthetic negative interactions with *set3*Δ were suppressed by relatively few of the query genes; only 7 of the 25 interactions were suppressed by more than 4 of the 6 suppressors. However, unlike the *htz1*Δ case, the *sgf11*Δ, and *ubp8*Δ suppressors in the H2B ubiquitination module stand out as interacting with a majority of the scored *set3*Δ interactions (Table 4 and Table S4). Taken together, these results argue that *htz1*Δ *set3*Δ has defects in chromatin function that are relatively restricted to that double mutant. These defects are bypassed by a set of suppressors that is also an uncommon constellation of genes suggesting a special functional relationship among *htz1*Δ, *set3*Δ, and their bypass suppressors.

High-copy suppressors of *htz1*Δ *set3*Δ genetic interaction: To gain further insights into the genetic interaction between *htz1*Δ and *set3*Δ, we performed a genome-wide screen to isolate high-copy suppressors of the *htz1*Δ *set3*Δ synthetic growth phenotype using a 2μ-plasmid-based systematic genomic library (JONES *et al.* 2008). Each clone of this library contains a sequenced fragment of the yeast chromosome and together they

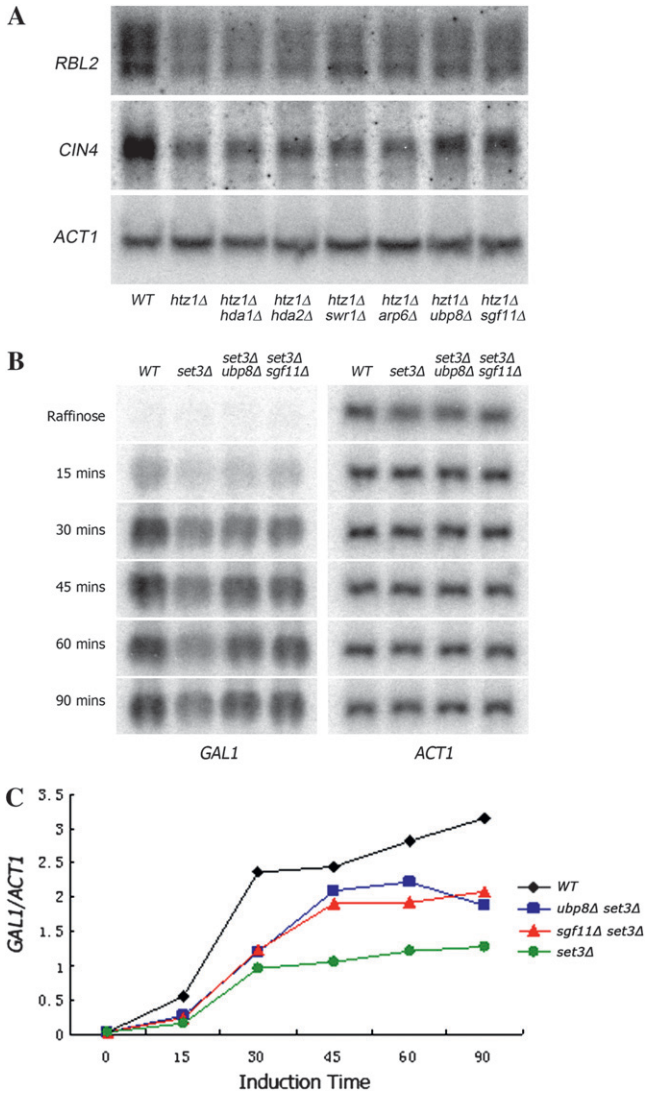

FIGURE 5.—Suppression of *htz1*Δ and *set3*Δ transcriptional phenotypes by *ubp8*Δ and *sgf11*Δ. (A) Total RNA (20 μg) isolated from each strain was subjected to Northern analysis. The membrane was blotted sequentially with probes that detect *RBL2*, *CIN4*, and *ACT1*. The membrane was stripped with boiling 0.1% SDS between each probing. (B) Northern analysis of 20 μg of total RNA from each strain is shown following galactose addition. The membrane was assayed sequentially with probes detecting *GAL1* and *ACT1*. (C) The ratios of *GAL1* mRNA to *ACT1* mRNA are shown across the course of induction of each strain.

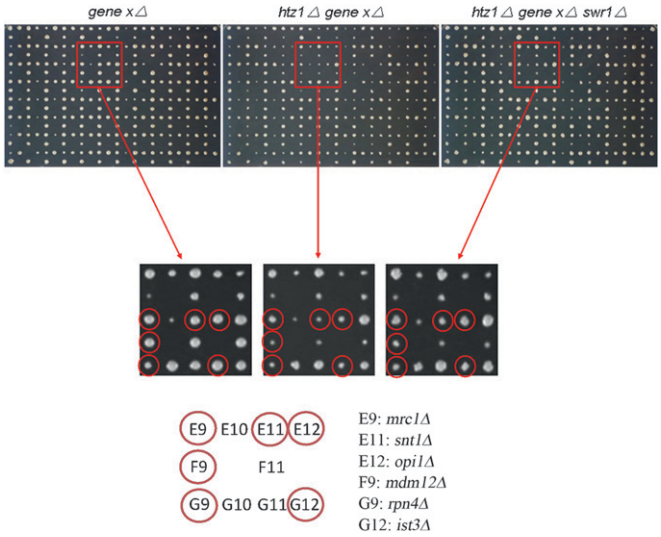

FIGURE 6.—SGA miniarray analysis. Three final ordered arrays from one set of the suppressor SGA experiments are shown. Crosses incorporating *swr1*Δ are used in this example, but similar assays were carried out for all of the suppressors tested. After colony sizes were first normalized across the plates using a set of control strains, synthetic negative gene interactions were scored by comparing plate A to plate B (MATERIALS AND METHODS). Bypass suppression was then scored as an increase in colony size of at least 33% comparing plate C to plate B. Reductions or increases in colony sizes can be visualized for the selected deletions showing interactions with *htz1*Δ. The enlarged areas show examples of suppression with the genes and their locations in the miniarray indicated. Note that *snt1* (E11) is one of the core subunits of the Set3 HDAC complex.

cover the complete *S. cerevisiae* genome. The library plasmids were used to transform MSY4544, which is MSY4474 containing a low-copy *SLX5* plasmid to enhance sensitivity. Leu$^+$ transformants were screened for color sectored colonies (MATERIALS AND METHODS) and five library plasmids showing strong suppression of *htz1*Δ *set3*Δ were recovered (data not shown). The promoter and ORF of each individual gene on these library plasmids were subcloned into a 2μ plasmid shuttle vector and tested individually in MSY4544. These assays identified the following high-copy suppressors (and the number of times they were isolated): *BDF1* (6), *AHC1* (2), *RMR1* (3), and *CYC8* (2). Suppression was independent of low-copy *SLX5* overexpression (Figure 7). The suppression of a fifth library plasmid could not be assigned to any single gene on the plasmid. Interestingly, this plasmid contains a copy of the *HMR* locus, which could theoretically serve as a titrator of Sir3 protein and mimic the suppression by *sir3*Δ. Since *BDF1* provided strong suppression, we also tested overexpression of *BDF2*, but it failed to confer suppression of the *htz1*Δ *set3*Δ synthetic phenotype (data not shown).

Suppression of *htz1*Δ and *set3*Δ single defects by high-copy suppressors: Loss-of-function suppressors differentially alleviate the single defects of *htz1*Δ or *set3*Δ cells and we attempted to characterize the high-copy suppressors using the same approach. Derivatives of the 2μ plasmid pRS425 containing *BDF1*, *AHC1*, *RMR1* and *CYC8* were introduced into *htz1*Δ cells and pRS425 empty vector was transformed as control. We then compared the sensitivities of these transformants to MMS, HU, and benomyl (Figure 8). *CYC8* overexpression notably suppresses the MMS sensitivity of *htz1*Δ but it has very subtle, if any, effects on the HU and benomyl sensitivities. This profile is similar to that observed earlier for deletions of genes encoding the Hda1 complex. Interestingly, Cyc8 forms a transcriptional corepressor complex with Tup1 and together they recruit the Hda1 complex to its targets (WU *et al.* 2001). Thus, *CYC8* overexpression could exert its dominant suppression by sequestering the Hda1 complex away from its physiological targets mimicking the disruption of the complex by the Hda1 complex gene deletions. Overexpression of *BDF1* exhibits a wide spectrum suppression of all of the *htz1*Δ phenotypes tested, while overexpression of *AHC1* and *RMR1* does not suppress any (Figure 8). In the case of *set3*Δ, the overexpression of *RMR1* markedly improves growth in the presence of MPA (Figure 9), suggesting a regulatory role of Rmr1 in transcription. We also observed that *BDF1* overexpression exacerbates the *set3*Δ MPA sensitivity.

DISCUSSION

The results reported here reveal a surprisingly close functional relationship between Htz1 and Set3 and suggest a model for Set3 activity. Synthetic growth defects for the binary combinations of both *htz1*Δ *set3*Δ and *swr1*Δ *set3*Δ are well known (KROGAN *et al.* 2003; COLLINS

TABLE 4

Suppression of genome-wide interactions of *htz1* and *set3*

	Number suppressed[a]	
Suppressors	*htz1* (164)	*set3* (25)
hda2	53	8
hda3	62	7
pre9	32	16
rpn10	40	7
sgf11	67	17
ubp8	58	20
*swr*1	55	N/A[b]
vps72	57	N/A[b]

[a] The total numbers of scored interactions are shown in parentheses.

[b] *swr1* and *vps72* are synthetic lethal in combination with *set3* in the background of BY4741.

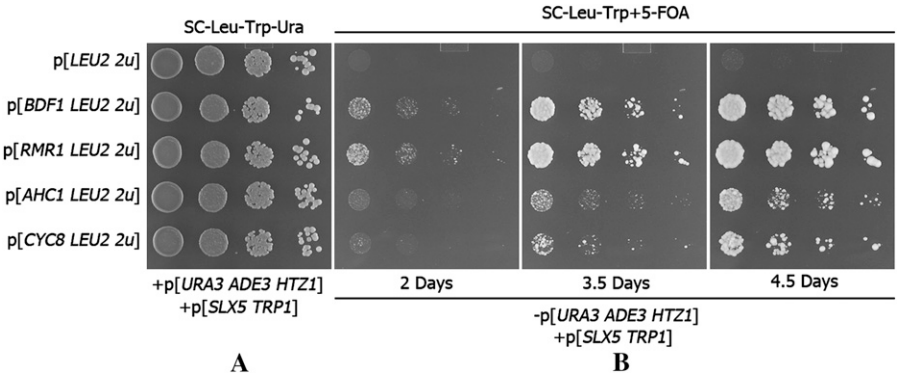

FIGURE 7.—(A) An *htz1*Δ *set3*Δ strain carrying pMSS59[*HTZ1 ADE3 URA3*] and pMH02[*SLX5 TRP1*] was transformed with the indicated plasmids. The transformants were cultured in SC–Ura–Leu–Trp media and serial dilutions were plated on SC–Ura–Leu–Trp plates to maintain the three plasmids. (B) Strains from A were then grown in SC–Leu–Trp media overnight to permit loss of pMSS59. Serial dilutions of the overnight cultures were plated on SC–Leu–Trp + 5-FOA plates. Growth at different times is shown.

et al. 2007; WILMES *et al.* 2008; COSTANZO *et al.* 2010). Furthermore, Swr1 is detrimental to cells in the absence of its normal Htz1–H2B substrate (HALLEY *et al.* 2010; MORILLO-HUESCA *et al.* 2010). What is surprising, then, is the striking finding that *htz1*Δ *swr1*Δ *set3*Δ triple mutants grow relatively well. This implies that not only is Swr1 severely detrimental in the absence of Htz1 and Set3, but Htz1 is also severely detrimental in the absence of Swr1 and Set3, a previously unrecognized activity of Htz1. Furthermore, the partial redundancy of these three genes is likely to be in a specific pathway of chromatin function since we find that the particular combination of suppressor genes that can bypass *htz1*Δ *set3*Δ is uncommon among the global set of *htz1*Δ synthetic interactions. This interlocking genetic relationship between *HTZ1*, *SWR1*, and *SET3* argues that Set3 may participate in the dynamic deposition and remodeling of Htz1-containing nucleosomes. In the absence of Htz1, we propose that the Set3 HDAC complex can partially overcome the effect of SWR1 complex either by decreasing its recruitment or modifying its target nucleosomes. In the absence of Swr1, we reason that Set3 activity may partially overcome either the negative effects of Htz1 nucleosomes no longer remodeled by the SWR1 complex or the stochastic misincorporation of Htz1 into abnormal sites of deposition.

The phenotypic characterization of our suppressor collection also revealed a surprising functional similarity between the SWR1 complex and the SAGA H2B deubiquitination subcomplex with respect to *htz1*Δ *set3*Δ. The simplest interpretation of these results is that the activities of these two complexes are partially redundant for achieving dynamic regulation of chromatin by Htz1. In the context of our experiments, the toxic effects of Swr1 in the absence of Htz1 might be relieved by the increased H2B ubiquitination in *ubp8*Δ or *sgf11*Δ mutants. This hypothesis is supported by the observation that H2B ubiquitination increases nucleosome stability over the promoters of repressed genes (CHANDRASEKHARAN *et al.* 2009). We carried out initial tests of this model by examining the steady-state levels of Htz1 at the promoters of repressed *GAL1* and *PHO5* by chromatin immunoprecipitation in *UBP8* and *ubp8*Δ cells. We also examined the rate of Htz1 deposition at the *PHO5* promoter following repression. Neither of these experiments revealed any effect of *ubp8*Δ on Htz1 occupancy (data not shown). However, both studies were carried out in the context of *HTZ1* and *SWR1* and it remains possible that *ubp8*Δ and *sgf11*Δ can relieve the detrimental Swr1-dependent remodeling of nucleosomes in the absence of Htz1. Alternatively, the Swr1 complex and the Ubp8–Sgf11 H2B deubiquitination subcomplex might function sequentially in a common pathway, although the downstream effect of this hypothetical pathway is unlikely to be Htz1 deposition.

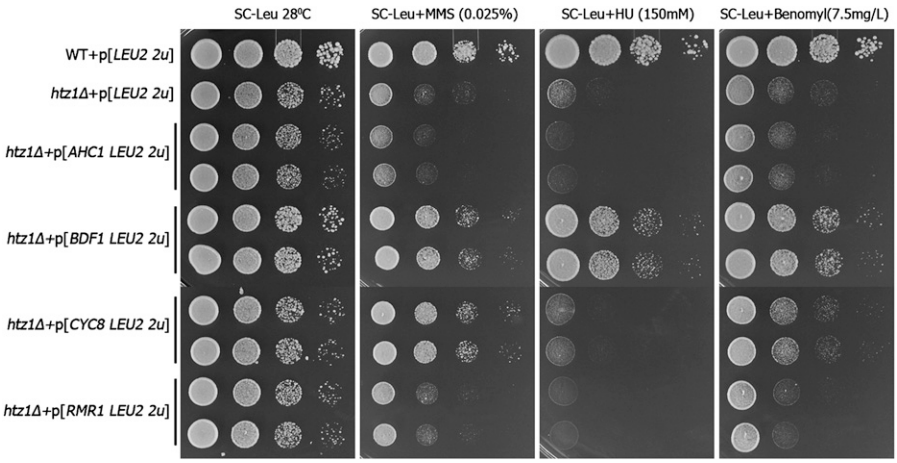

FIGURE 8.—Suppression of *htz1*Δ drug sensitivities by high-copy suppressors. Serial dilutions of the cell cultures of *htz1*Δ cells containing the indicated plasmids were plated on SC–Leu, SC–Leu + MMS (0.025%), SC–Leu + hydroxyurea (150 mM) and SC–Leu + benomyl (7.5 μg/ml).

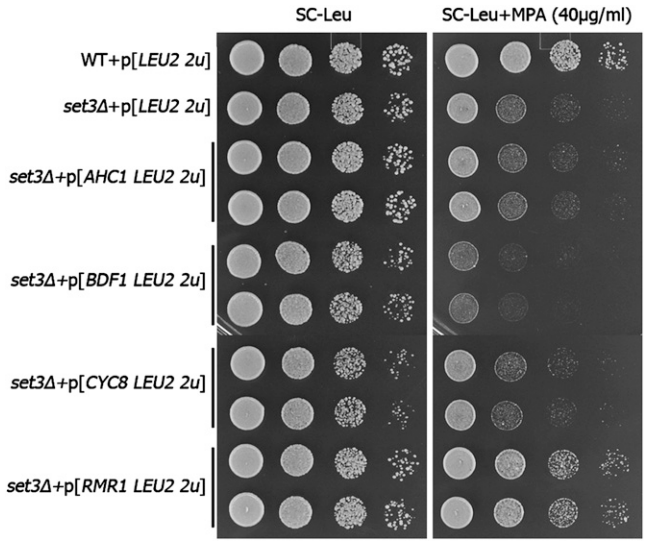

Figure 9.—Suppression of *set3*Δ drug sensitivities by high-copy suppressors. Serial dilutions of *set3*Δ cells containing the indicated plasmids were plated on SC–Leu, SC–Leu + MPA (40 μg/ml).

Our suppressor analysis also revealed a second functional similarity between Sir3 and the proteasome protein degradation pathway. Overexpression of *SIR3* not only reduced *htz1*Δ *set3*Δ suppression by *set1*, but also antagonized suppression by *rpn10*Δ, *pre9*Δ, and *ubp14*Δ. Furthermore, we also found that telomere silencing is impaired in *rpn10*Δ, *pre9*Δ, and *ubp14*Δ, just as it is in *sir3*Δ. A number of links between protein degradation and silencing are known. Physical interactions have been reported between the ubiquitin-specific protease Ubp3 and Sir4, and increased telomere silencing was observed in *ubp3*Δ (Moazed and Johnson 1996). Another ubiquitin protease, Ubp6, and the proteasome subunit Sem1 are also involved in telomere silencing. Silencing is reduced in *sem1*Δ, suggesting a positive role in silencing, while defective silencing in *ubp10*Δ is rescued by *ubp6*Δ, suggesting a negative role for Ubp6 (Qin *et al.* 2009). Our results suggest additional functional overlaps between the proteasome, ubiquitin recycling, and Sir3-dependent silencing.

It was curious that the deletion of genes encoding the HDA1 deacetylase complex would bypass defects involving the deletion *set3*Δ, which is a subunit of a deacetylase complex. However, a similar antagonism between the HDA1 and HOS2 deacetylases has recently been observed in *Candida albicans* (Zacchi *et al.* 2010). HDA1 specifically deacetylates H2B and H3 and, in its absence, intergenic promoter regions and so-called HDA1-affected subtelomeric regions (HAST) become hyperacetylated (Robyr *et al.* 2002). Interestingly, HDA1 is a downstream effector of the Tup1–Cyc8 repressor complex, establishing transcriptionally repressive chromatin at promoter regions (Wu *et al.* 2001; Green and Johnson 2004). Furthermore, Tup1 likely participates in specifying some of the sites of Htz1 deposition by SWR1 (Gligoris *et al.* 2007). Although we did not recover *tup1*Δ in our suppressor screens, the fact that *CYC8* is a high-copy suppressor suggests that reducing HDA1 activity at its Tup1-independent targets might contribute to the suppression of *htz1*Δ *set3*Δ.

The functional involvement of Slx5–Slx8 in the Htz1 and Set3 network is provocative. *SLX5* was previously recovered in a systematic study of overexpression toxicity (Sopko *et al.* 2006). Interestingly, *SLX5* overexpression specifically blocks the ability of deletions in genes encoding SWR1 and the SAGA H2B deubiquitination subcomplex to suppress the growth phenotype of *htz1*Δ *set3*Δ. We reason that overexpression of *SLX5* increases the polyubiquitination and degradation of one or more target proteins critical for growth in the suppression genotypes. Given the DNA damage sensitivity of *htz1*Δ, and the roles of H2B ubiquitination in repair (Lis and Romesberg 2006; Game and Chernikova 2009), one potential pathway for these targets is DNA damage repair. Nagai *et al.* (2008) have proposed that Slx5–Slx8 is required to target degradation of an unknown SUMOylated factor that must be removed for repair to proceed. Thus, excess degradation could be lethal in *htz1*Δ *set3*Δ regardless of the altered chromatin structure provided by *swr1*Δ or *ubp8*Δ. Transcription initiation is a second candidate pathway. Temperature-sensitive *mot1-301*, which cannot efficiently dissociate TATA-binding protein from the promoter DNA, is suppressed by *slx5*Δ (Wang *et al.* 2006). This model suggests that Slx5–Slx8 polyubiquitinates an unknown SUMOylated protein that enhances transcription initiation and that the increased concentration of this factor in the *slx5*Δ can suppress the *mot1-301* defect. Because *SLX5* overexpression diminishes the beneficial effects of disrupting either SWR1 complex or Ubp8–Sgf11 in *htz1*Δ *set3*Δ and because both Htz1-containing nucleosomes and Set3 HDAC modified nucleosomes are promoter proximal (Albert *et al.* 2007; Kim and Buratowski 2009), the transcription initiation pathway is an attractive model for the targets of Slx5–Slx8 in our network.

Both models predict that overexpression of genes encoding Slx5–Slx8 substrates might relieve the negative effect of increased *SLX5* dosage and that the proteins expressed should be SUMOylated. Both Bdf1 and Rmr1 have been isolated in proteomics screens for SUMOylated proteins (Wohlschlegel *et al.* 2004; Hannich *et al.* 2005; Yu *et al.* 2008). As a component of SWR1, increased Slx5–Slx8 targeted degradation of Bdf1 might further impair transcription in *htz1*Δ *set3*Δ. Overexpression of *BDF1* would compensate for this increased degradation. Furthermore, high-copy *BDF1* might confer additional suppression by diluting SWR1 complex and mimicking suppression by *swr1*Δ. However, the mechanism is likely to be more complicated since the suppression of *htz1*Δ phenotypes by *BDF1* is more extensive than that achieved

by *swr1*Δ. Indeed, Bdf1 is more widely distributed across chromosomes than would be expected on the basis of its association with TFIID and SWR1 (Chua and Roeder 1995; Matangkasombut and Buratowski 2003). In the case of *RMR1*, relatively little is known about its functions, although our results suggest a potential role in transcription. Interestingly, *RMR1* is a weak high-copy suppressor of the null allele of *ulp2*, one of two essential SUMO proteases in budding yeast (Hannich *et al.* 2005).

Expanding the binary synthetic *htz1*Δ *set3*Δ interaction to a network of ternary gene interactions has revealed strong functional links among a small set of protein complexes with general regulatory functions. Importantly, these results suggest an important new role for the Set3 HDAC complex in Htz1–nucleosome dynamics. Further genetic, biochemical, and molecular studies will help to dissect these interactions at a mechanistic level, providing new insights into the epigenetic regulation of chromatin function.

This work was supported by a Robert R. Wagner Fellowship to M.H. and grants GM28920 and GM60444 from the National Institutes of Health to M.M.S.

LITERATURE CITED

Adams, A., C. Kaiser and C. S. H. Laboratory, 1998 *Methods in Yeast Genetics: A Cold Spring Harbor Laboratory Course Manual*. Cold Spring Harbor Laboratory Press, Plainview, NY.

Albert, I., T. N. Mavrich, L. P. Tomsho, J. Qi, S. J. Zanton *et al.*, 2007 Translational and rotational settings of H2A.Z nucleosomes across the *Saccharomyces cerevisiae* genome. Nature **446:** 572–576.

Altaf, M., A. Auger, J. Monnet-Saksouk, J. Brodeur, S. Piquet *et al.*, 2010 NuA4-dependent acetylation of nucleosomal histones H4 and H2A directly stimulates incorporation of H2A.Z by the SWR1 complex. J. Biol. Chem. **285:** 15966–15977.

Barski, A., S. Cuddapah, K. Cui, T. Y. Roh, D. E. Schones *et al.*, 2007 High-resolution profiling of histone methylations in the human genome. Cell **129:** 823–837.

Bender, A., and J. R. Pringle, 1991 Use of a screen for synthetic lethal and multicopy suppressee mutants to identify two new genes involved in morphogenesis in *Saccharomyces cerevisiae*. Mol. Cell Biol. **11:** 1295–1305.

Burgess, R. C., S. Rahman, M. Lisby, R. Rothstein and X. Zhao, 2007 The Slx5–Slx8 complex affects sumoylation of DNA repair proteins and negatively regulates recombination. Mol. Cell Biol. **27:** 6153–6162.

Chandrasekharan, M. B., F. Huang and Z. W. Sun, 2009 Ubiquitination of histone H2B regulates chromatin dynamics by enhancing nucleosome stability. Proc. Natl. Acad. Sci. USA **106:** 16686–16691.

Chua, P., and G. S. Roeder, 1995 Bdf1, a yeast chromosomal protein required for sporulation. Mol. Cell Biol. **15:** 3685–3696.

Cohen, T. J., M. J. Mallory, R. Strich and T. P. Yao, 2008 Hos2p/Set3p deacetylase complex signals secretory stress through the mpk1p cell integrity pathway. Eukaryot. Cell **7:** 1191–1199.

Collins, S. R., K. M. Miller, N. L. Maas, A. Roguev, J. Fillingham *et al.*, 2007 Functional dissection of protein complexes involved in yeast chromosome biology using a genetic interaction map. Nature **446:** 806–810.

Costanzo, M., A. Baryshnikova, J. Bellay, Y. Kim, E. D. Spear *et al.*, 2010 The genetic landscape of a cell. Science **327:** 425–431.

Creyghton, M. P., S. Markoulaki, S. S. Levine, J. Hanna, M. A. Lodato *et al.*, 2008 H2AZ is enriched at polycomb complex target genes in es cells and is necessary for lineage commitment. Cell **135:** 649–661.

Cui, K., C. Zang, T. Y. Roh, D. E. Schones, R. W. Childs *et al.*, 2009 Chromatin signatures in multipotent human hematopoietic stem cells indicate the fate of bivalent genes during differentiation. Cell. Stem Cell **4:** 80–93.

Darst, R. P., S. N. Garcia, M. R. Koch and L. Pillus, 2008 Slx5 promotes transcriptional silencing and is required for robust growth in the absence of Sir2. Mol. Cell Biol. **28:** 1361–1372.

Dhillon, N., M. Oki, S. J. Szyjka, O. M. Aparicio and R. T. Kamakaka, 2006 H2A.Z functions to regulate progression through the cell cycle. Mol. Cell Biol. **26:** 489–501.

Fiedler, D., H. Braberg, M. Mehta, G. Chechik, G. Cagney *et al.*, 2009 Functional organization of the *S. cerevisiae* phosphorylation network. Cell **136:** 952–963.

Game, J. C., and S. B. Chernikova, 2009 The role of *RAD6* in recombinational repair, checkpoints and meiosis via histone modification. DNA Repair **8:** 470–482.

Giaever, G., A. M. Chu, L. Ni, C. Connelly, L. Riles *et al.*, 2002 Functional profiling of the *Saccharomyces cerevisiae* genome. Nature **418:** 387–391.

Gligoris, T., G. Thireos and D. Tzamarias, 2007 The Tup1 corepressor directs Htz1 deposition at a specific promoter nucleosome marking the *GAL1* gene for rapid activation. Mol. Cell Biol. **27:** 4198–4205.

Govind, C. K., H. Qiu, D. S. Ginsburg, C. Ruan, K. Hofmeyer *et al.*, 2010 Phosphorylated Pol II CTD recruits multiple HDACs, including Rpd3C(S), for methylation-dependent deacetylation of ORF nucleosomes. Mol. Cell **39:** 234–246.

Green, S. R., and A. D. Johnson, 2004 Promoter-dependent roles for the Srb10 cyclin-dependent kinase and the Hda1 deacetylase in Tup1-mediated repression in *Saccharomyces cerevisiae*. Mol. Biol. Cell **15:** 4191–4202.

Guenther, M. G., W. S. Lane, W. Fischle, E. Verdin, M. A. Lazar *et al.*, 2000 A core SMRT corepressor complex containing HDAC3 and TBL1, a WD40-repeat protein linked to deafness. Genes Dev. **14:** 1048–1057.

Guillemette, B., A. R. Bataille, N. Gevry, M. Adam, M. Blanchette *et al.*, 2005 Variant histone H2A.Z is globally localized to the promoters of inactive yeast genes and regulates nucleosome positioning. PLoS Biol. **3:** e384.

Halley, J. E., T. Kaplan, A. Y. Wang, M. S. Kobor and J. Rine, 2010 Roles for H2A.Z and its acetylation in *GAL1* transcription and gene induction, but not *GAL1*-transcriptional memory. PLoS Biol. **8:** e1000401.

Hannich, J. T., A. Lewis, M. B. Kroetz, S. J. Li, H. Heide *et al.*, 2005 Defining the SUMO-modified proteome by multiple approaches in *Saccharomyces cerevisiae*. J. Biol. Chem. **280:** 4102–4110.

John, S., P. J. Sabo, T. A. Johnson, M. H. Sung, S. C. Biddie *et al.*, 2008 Interaction of the glucocorticoid receptor with the chromatin landscape. Mol. Cell **29:** 611–624.

Jones, G. M., J. Stalker, S. Humphray, A. West, T. Cox *et al.*, 2008 A systematic library for comprehensive overexpression screens in *Saccharomyces cerevisiae*. Nat. Methods **5:** 239–241.

Kahana, A., and D. E. Gottschling, 1999 *DOT4* links silencing and cell growth in *Saccharomyces cerevisiae*. Mol. Cell Biol. **19:** 6608–6620.

Kim, T., and S. Buratowski, 2009 Dimethylation of H3K4 by Set1 recruits the Set3 histone deacetylase complex to 5′ transcribed regions. Cell **137:** 259–272.

Kobor, M. S., S. Venkatasubrahmanyam, M. D. Meneghini, J. W. Gin, J. L. Jennings *et al.*, 2004 A protein complex containing the conserved Swi2/Snf2-related ATPase Swr1p deposits histone variant H2A.Z into euchromatin. PLoS Biol. **2:** E131.

Krogan, N. J., M. C. Keogh, N. Datta, C. Sawa, O. W. Ryan *et al.*, 2003 A Snf2 family ATPase complex required for recruitment of the histone H2A variant Htz1. Mol. Cell **12:** 1565–1576.

Li, B., S. G. Pattenden, D. Lee, J. Gutierrez, J. Chen *et al.*, 2005 Preferential occupancy of histone variant H2AZ at inactive promoters influences local histone modifications and chromatin remodeling. Proc. Natl. Acad. Sci. USA **102:** 18385–18390.

Li, J., J. Wang, Z. Nawaz, J. M. Liu, J. Qin *et al.*, 2000 Both corepressor proteins SMRT and N-CoR exist in large protein complexes containing HDAC3. EMBO J. **19:** 4342–4350.

Li, T., J. Fung, J. R. Mullen and S. J. Brill, 2007a The yeast Slx5-Slx8 DNA integrity complex displays ubiquitin ligase activity. Cell Cycle **6:** 2800–2809.

Li, T., J. R. Mullen, C. E. Slagle and S. J. Brill, 2007b Stimulation of in vitro sumoylation by Slx5-Slx8: evidence for a functional interaction with the SUMO pathway. DNA Repair **6:** 1679–1691.

Lin, Y. Y., Y. Qi, J. Y. Lu, X. Pan, D. S. Yuan *et al.*, 2008 A comprehensive synthetic genetic interaction network governing yeast histone acetylation and deacetylation. Genes Dev. **22:** 2062–2074.

Lis, E. T., and F. E. Romesberg, 2006 Role of Doa1 in the *Saccharomyces cerevisiae* DNA damage response. Mol. Cell Biol. **26:** 4122–4133.

Matangkasombut, O., and S. Buratowski, 2003 Different sensitivities of bromodomain factors 1 and 2 to histone H4 acetylation. Mol. Cell **11:** 353–363.

Mavrich, T. N., C. Jiang, I. P. Ioshikhes, X. Li, B. J. Venters *et al.*, 2008 Nucleosome organization in the Drosophila genome. Nature **453:** 358–362.

McKenna, N. J., and B. W. O'Malley, 2002 Combinatorial control of gene expression by nuclear receptors and coregulators. Cell **108:** 465–474.

Meneghini, M. D., M. Wu and H. D. Madhani, 2003 Conserved histone variant H2A.Z protects euchromatin from the ectopic spread of silent heterochromatin. Cell **112:** 725–736.

Mizuguchi, G., X. Shen, J. Landry, W. H. Wu, S. Sen *et al.*, 2004 ATP-driven exchange of histone H2AZ variant catalyzed by SWR1 chromatin remodeling complex. Science **303:** 343–348.

Moazed, D., and D. Johnson, 1996 A deubiquitinating enzyme interacts with Sir4 and regulates silencing in *S. cerevisiae*. Cell **86:** 667–677.

Morillo-Huesca, M., M. Clemente-Ruiz, E. Andujar and F. Prado, 2010 The SWR1 histone replacement complex causes genetic instability and genome-wide transcription misregulation in the absence of H2A. Z. PLoS One **5:** e12143.

Mullen, J. R., and S. J. Brill, 2008 Activation of the Slx5-Slx8 ubiquitin ligase by poly-small ubiquitin-like modifier conjugates. J. Biol. Chem. **283:** 19912–19921.

Nagai, S., K. Dubrana, M. Tsai-Pflugfelder, M. B. Davidson, T. M. Roberts *et al.*, 2008 Functional targeting of DNA damage to a nuclear pore-associated SUMO-dependent ubiquitin ligase. Science **322:** 597–602.

Nixon, C. E., A. J. Wilcox and J. D. Laney, 2010 Degradation of the *Saccharomyces cerevisiae* mating-type regulator alpha1: genetic dissection of *cis*-determinants and *trans*-acting pathways. Genetics **185:** 497–511.

Ooi, S. L., D. D. Shoemaker and J. D. Boeke, 2003 DNA helicase gene interaction network defined using synthetic lethality analyzed by microarray. Nat. Genet. **35:** 277–286.

Pan, X., P. Ye, D. S. Yuan, X. Wang, J. S. Bader *et al.*, 2006 A DNA integrity network in the yeast *Saccharomyces cerevisiae*. Cell **124:** 1069–1081.

Pijnappel, W. W., D. Schaft, A. Roguev, A. Shevchenko, H. Tekotte *et al.*, 2001 The *S. cerevisiae* Set3 complex includes two histone deacetylases, Hos2 and Hst1, and is a meiotic-specific repressor of the sporulation gene program. Genes Dev. **15:** 2991–3004.

Qin, S., Q. Wang, A. Ray, G. Wani, Q. Zhao *et al.*, 2009 Sem1p and Ubp6p orchestrate telomeric silencing by modulating histone H2B ubiquitination and H3 acetylation. Nucleic Acids Res. **37:** 1843–1853.

Raisner, R. M., P. D. Hartley, M. D. Meneghini, M. Z. Bao, C. L. Liu *et al.*, 2005 Histone variant H2A.Z marks the 5′ ends of both active and inactive genes in euchromatin. Cell **123:** 233–248.

Rangasamy, D., I. Greaves and D. J. Tremethick, 2004 RNA interference demonstrates a novel role for H2A.Z in chromosome segregation. Nat. Struct. Mol. Biol. **11:** 650–655.

Robyr, D., Y. Suka, I. Xenarios, S. K. Kurdistani, A. Wang *et al.*, 2002 Microarray deacetylation maps determine genome-wide functions for yeast histone deacetylases. Cell **109:** 437–446.

Ross-MacDonald, P., A. Sheehan, C. Friddle, G. S. Roeder and M. Snyder, 1999 Transposon mutagenesis for the analysis of protein production, function, and localization. Methods Enzymol. **303:** 512–532.

Rundlett, S. E., A. A. Carmen, R. Kobayashi, S. Bavykin, B. M. Turner *et al.*, 1996 Hda1 and Rpd3 are members of distinct yeast histone deacetylase complexes that regulate silencing and transcription. Proc. Natl. Acad. Sci. USA **93:** 14503–14508.

Santisteban, M. S., T. Kalashnikova and M. M. Smith, 2000 Histone H2A.Z regulats transcription and is partially redundant with nucleosome remodeling complexes. Cell **103:** 411–422.

Sopko, R., D. Huang, N. Preston, G. Chua, B. Papp *et al.*, 2006 Mapping pathways and phenotypes by systematic gene overexpression. Mol. Cell **21:** 319–330.

Sutcliffe, E. L., I. A. Parish, Y. Q. He, T. Juelich, M. L. Tierney *et al.*, 2009 Dynamic histone variant exchange accompanies gene induction in T cells. Mol. Cell Biol. **29:** 1972–1986.

Swaminathan, J., E. M. Baxter and V. G. Corces, 2005 The role of histone H2Av variant replacement and histone H4 acetylation in the establishment of Drosophila heterochromatin. Genes Dev. **19:** 65–76.

Tong, A. H., M. Evangelista, A. B. Parsons, H. Xu, G. D. Bader *et al.*, 2001 Systematic genetic analysis with ordered arrays of yeast deletion mutants. Science **294:** 2364–2368.

Tong, A. H., G. Lesage, G. D. Bader, H. Ding, H. Xu *et al.*, 2004 Global mapping of the yeast genetic interaction network. Science **303:** 808–813.

Venkatasubrahmanyam, S., W. W. Hwang, M. D. Meneghini, A. H. Tong and H. D. Madhani, 2007 Genome-wide, as opposed to local, antisilencing is mediated redundantly by the euchromatic factors Set1 and H2A. Z. Proc. Natl. Acad. Sci. USA **104:** 16609–16614.

Wang, A., S. K. Kurdistani and M. Grunstein, 2002 Requirement of Hos2 histone deacetylase for gene activity in yeast. Science **298:** 1412–1414.

Wang, Z., and G. Prelich, 2009 Quality control of a transcriptional regulator by SUMO-targeted degradation. Mol. Cell Biol. **29:** 1694–1706.

Wang, Z., G. M. Jones and G. Prelich, 2006 Genetic analysis connects Slx5 and Slx8 to the SUMO pathway in *Saccharomyces cerevisiae*. Genetics **172:** 1499–1509.

Whittle, C. M., K. N. McClinic, S. Ercan, X. Zhang, R. D. Green *et al.*, 2008 The genomic distribution and function of histone variant htz-1 during *C. elegans* embryogenesis. PLoS Genet. **4:** e1000187.

Wilmes, G. M., M. Bergkessel, S. Bandyopadhyay, M. Shales, H. Braberg *et al.*, 2008 A genetic interaction map of RNA-processing factors reveals links between Sem1/Dss1-containing complexes and mRNA export and splicing. Mol. Cell **32:** 735–746.

Wohlschlegel, J. A., E. S. Johnson, S. I. Reed and J. R. Yates, 3rd, 2004 Global analysis of protein sumoylation in *Saccharomyces cerevisiae*. J. Biol. Chem. **279:** 45662–45668.

Wu, J., N. Suka, M. Carlson and M. Grunstein, 2001 Tup1 utilizes histone H3/H2B-specific Hda1 deacetylase to repress gene activity in yeast. Mol. Cell **7:** 117–126.

Xie, Y., E. M. Rubenstein, T. Matt and M. Hochstrasser, 2010 SUMO-independent in vivo activity of a SUMO-targeted ubiquitin ligase toward a short-lived transcription factor. Genes Dev. **24:** 893–903.

Yu, H., P. Braun, M. A. Yildirim, I. Lemmens, K. Venkatesan *et al.*, 2008 High-quality binary protein interaction map of the yeast interactome network. Science **322:** 104–110.

Yu, J., Y. Li, T. Ishizuka, M. G. Guenther and M. A. Lazar, 2003 A SANT motif in the SMRT corepressor interprets the histone code and promotes histone deacetylation. EMBO J. **22:** 3403–3410.

Zacchi, L. F., W. L. Schulz and D. A. Davis, 2010 HOS2 and HDA1 encode histone deacetylases with opposing roles in Candida albicans morphogenesis. PLoS One **5:** e12171.

Zhang, C., T. M. Roberts, J. Yang, R. Desai and G. W. Brown, 2006 Suppression of genomic instability by Slx5 and Slx8 in *Saccharomyces cerevisiae*. DNA Repair **5:** 336–346.

Zhang, H., D. N. Roberts and B. R. Cairns, 2005 Genome-wide dynamics of Htz1, a histone H2A variant that poises repressed/basal promoters for activation through histone loss. Cell **123:** 219–231.

Zilberman, D., D. Coleman-Derr, T. Ballinger and S. Henikoff, 2008 Histone H2A.Z and DNA methylation are mutually antagonistic chromatin marks. Nature **456:** 125–129.

Communicating editor: F. Winston

GENETICS

Supporting Information
http://www.genetics.org/cgi/content/full/genetics.110.125419/DC1

Genetic Analysis Implicates the Set3/Hos2 Histone Deacetylase in the Deposition and Remodeling of Nucleosomes Containing H2A.Z

Mingda Hang and M. Mitchell Smith

DOI: 10.1534/genetics.110.125419

TABLE S1

*htz1*Δ mini-array spreadsheet

Table S1 is available as an Excel file at http://www.genetics.org/cgi/content/full/genetics.110.125419/DC1.

TABLE S2

***set3*Δ mini-array spreadsheet**

GENE	ORF	BATCH[1]	ROW[2]	COL[3]	Comment[4]	ROW[5]	COL[6]
	YAL037W				control	C	3
	YAL037W				control	C	4
APQ12	YIL040W	2	D	1		C	5
APQ12	YIL040W					C	6
ARD1	YHR013C	2	C	7		C	7
ARD1	YHR013C					C	8
ARP6	YLR085C	chr12_2	E	8		C	9
ARP6	YLR085C					C	10
CDC73	YLR418C	2	H	9		C	11
CDC73	YLR418C					C	12
CIK1	YMR198W	chr00_11	G	7		C	13
CIK1	YMR198W					C	14
CSE2	YNR010W	3	B	11		C	15
CSE2	YNR010W					C	16
CSM1	YCR086W	1	D	1		C	17
CSM1	YCR086W					C	18
CTI6	YPL181W	3	G	8		C	19
CTI6	YPL181W					C	20
DEP1	YAL013W	1	A	3		C	21
DEP1	YAL013W					C	22
ARD1	YHR013C					D	7
ARP6	YLR085C					D	9
CDC73	YLR418C					D	11
CIK1	YMR198W					D	13
CSE2	YNR010W					D	15
CSM1	YCR086W					D	17
CTI6	YPL181W					D	19

GIM3	YNL153C	3	B	4		E	3
GIM3	YNL153C					E	4
GCR2	YNL199C	chr14_2	D	9		E	5
GCR2	YNL199C					E	6
ERG3	YLR056W	chr14_2	D	9		E	7
ERG3	YLR056W					E	8
SED4	YCR067C				control	E	9
SED4	YCR067C				control	E	10
GIM4	YEL003W	1	G	9		E	11
GIM4	YEL003W					E	12
HCM1	YCR065W	1	C	8		E	13
HCM1	YCR065W					E	14
HCS1	YKL017C	chr11_1	B	6		E	15
HCS1	YKL017C					E	16
HTZ1	YOL012C	chr15_5	B	11		E	17
HTZ1	YOL012C					E	18
LGE1	YPL055C	3	F	12		E	19
LGE1	YPL055C					E	20
MDM35	YKL053C-A	3	F	12		E	21
MDM35	YKL053C-A					E	22
GIM3	YNL153C					F	3
GCR2	YNL199C					F	5
ERG3	YLR056W					F	7
SED4	YCR067C				control	F	9
GIM4	YEL003W					F	11
HCM1	YCR065W					F	13
HCS1	YKL017C					F	15
HTZ1	YOL012C					F	17
LGE1	YPL055C					F	19

MET13	YGL125W				control	G	3
MET13	YGL125W				control	G	4
MFT1	YML062C	chr13_1	G	4		G	5
MFT1	YML062C					G	6
PAC10	YGR078C	2	B	10		G	7
PAC10	YGR078C					G	8
PFD1	YJL179W	2	E	8		G	9
PFD1	YJL179W					G	10
PHO23	YNL097C	3	A	11		G	11
PHO23	YNL097C					G	12
RGP1	YDR137W	1	E	3		G	13
RGP1	YDR137W					G	14
PDE1	YGL248W				control	G	15
PDE1	YGL248W				control	G	16
RIC1	YLR039C	2	G	5		G	17
RIC1	YLR039C					G	18
RPD3	YNL330C	3	B	10		G	19
RPD3	YNL330C					G	20
RXT2	YBR095C	1	B	1		G	21
RXT2	YBR095C					G	22
MET13	YGL125W				control	H	3
MFT1	YML062C					H	5
PAC10	YGR078C					H	7
PFD1	YJL179W					H	9
PHO23	YNL097C					H	11
RGP1	YDR137W					H	13
PDE1	YGL248W				control	H	15
RIC1	YLR039C					H	17
RPD3	YNL330C					H	19

RXT2	YBR095C					H	21
SAP30	YMR263W	3	A	7		I	3
SAP30	YMR263W					I	4
SDS3	YIL084C	2	D	2		I	5
SDS3	YIL084C					I	6
SEC22	YLR268W	chr12_4	D	5		I	7
SEC22	YLR268W					I	8
	YGR176W				control	I	9
	YGR176W				control	I	10
SET2	YJL168C	2	E	4		I	11
SET2	YJL168C					I	12
SIN3	YOL004W	3	C	1		I	13
SIN3	YOL004W					I	14
SLM3	YDL033C	chr4_1	C	9		I	15
SLM3	YDL033C					I	16
SNF5	YBR289W	chr00_16	B	11		I	17
SNF5	YBR289W					I	18
SNU66	YOR308C	3	F	5		I	19
SNU66	YOR308C					I	20
	YJL021C				control	I	21
	YJL021C				control	I	22
SAP30	YMR263W					J	3
SDS3	YIL084C					J	5
SEC22	YLR268W					J	7
	YGR176W				control	J	9
SET2	YJL168C					J	11
SIN3	YOL004W					J	13
SLM3	YDL033C					J	15
SNF5	YBR289W					J	17

SNU66	YOR308C					J	19
	YJL021C				control	J	21
SWC5	YBR231C	chr2_4	E	11		K	13
SWC5	YBR231C					K	14
SFH1	YKL091C				control	K	15
SFH1	YKL091C				control	K	16
SWR1	YDR334W	chr4_6	H	9		K	17
SWR1	YDR334W					K	18
THP2	YHR167W	chr8_3	C	5		K	19
THP2	YHR167W					K	20
TIM18	YOR297C	chr15_4	A	9		K	21
TIM18	YOR297C					K	22
SUB1	YMR039C					L	9
SWC3	YAL011W					L	11
SWC5	YBR231C					L	13
SFH1	YKL091C				control	L	15
SWR1	YDR334W					L	17
THP2	YHR167W					L	19
TIM18	YOR297C					L	21
TUB3	YML124C	3	A	3		M	3
TUB3	YML124C					M	4
UME6	YDR207C					M	10
VPS71	YML041C	chr00_11	E	7		M	11
VPS71	YML041C					M	12
VPS72	YDR485C	chr4_8	D	11		M	13
VPS72	YDR485C					M	14
VPS8	YAL002W	1	A	2		M	15
VPS8	YAL002W					M	16
YAF9	YNL107W	chr00_16	H	4		M	17

YAF9	YNL107W				M	18
YKE2	YLR200W	2	G	12	M	19
YKE2	YLR200W				M	20
YPT6	YLR262C	2	H	3	M	21
YPT6	YLR262C				M	22
TUB3	YML124C				N	3
UME6	YDR207C				N	9
VPS71	YML041C				N	11
VPS72	YDR485C				N	13
VPS8	YAL002W				N	15
YPT6	YLR262C				N	21

1,2,3: "Batch" "Row" and "Col" combined are the location of each deletion strain in the yeast deletion collection.

4: The control strains are indicated in "comment"

5, 6: Row and Col combined indicate the location of the deletion strain in the mini-library after being transferred to from the deletion collection

TABLE S3

***htz1*Δ genetic interactions suppressed by the *htz1*Δ *set3*Δ suppressors**

Suppressor	Synthetic Lethal Genes Suppressed (Growth Cutoff = 1.5)
hda1	YAL002W,YFR010W,YGL115W,YML124C,YMR263W,YMR272C,YNL021W,YNL097C,YBR095C,YGL244W,YGR056W,YGR063C,YBR279W,YGR078C,YCL008C,YNL148C,YNL153C,YNL229C,YNR010W,YCL037C,YHL011C,YHR013C,YHR041C,YCR081W,YIL020C,YIL084C,YDL013W,YDL020C,YIR005W,YJL006C,YJL127C,YOL115W,YJL140W,YDR159W,YDR207C,YJL179W,YOR026W,YOR123C,YKL204W,YKL213C,YOR141C,YDR448W,YKR029C,YLL027W,YLR055C,YLR200W,YPL181W,YPL182C,YER070W,YPR031W,YPR057W,YPR070W,YPR120C
hda2	YFR010W,YGL019W,YGL115W,YGL127C,YMR060C,YMR263W,YMR272C,YNL021W,YNL097C,YBR095C,YGL244W,YGR057C,YBR248C,YGR063C,YBR279W,YGR078C,YCL008C,YNL148C,YNL153C,YNL229C,YHL011C,YCR033W,YHR013C,YHR041C,YCR077C,YCR081W,YIL020C,YIL040W,YIL084C,YDL013W,YIL112W,YDL020C,YIR005W,YJL006C,YJL124C,YJL127C,YOL072W,YOL115W,YOR005C,YDR121W,YJL140W,YJL140W,YDR159W,YJL179W,YJR060W,YOR043W,YJR102C,YDR360W,YDR392W,YDR424C,YKL204W,YPL042C,YDR448W,YKR029C,YDR469W,YLL027W,YLR200W,YPL086C,YPL181W,YPL182C,YPR070W,YPR120C
pre9	YAL002W,YFR010W,YAL013W,YGL019W,YAL021C,YAR003W,YBL058W,YGL115W,YGL127C,YMR263W,YNL025C,YBR095C,YGL244W,YGR063C,YNL153C,YHL011C,YHR013C,YHR091C,YIL020C,YDL013W,YIR005W,YDL115C,YJL127C,YOL115W,YJL129C,YDR207C,YOR123C, YKL139W,YPL055C,YLR200W,YPR070W,YPR120C
rpn10	YFR010W,YAL021C,YGL115W,YGL127C,YMR263W,YNL097C,YNL136W,YBR095C,YGL244W,YGR057C,YBR279W,YGR188C,YNL153C,YNR010W,YCL037C,YHL011C,YHR013C,YCR081W,YIL020C,YIL040W,YIL084C,YIR005W,YJL127C,YOR005C,YJL129C,YJL140W,YJL179W,YJR060W,YOR043W,YOR123C,YDR318W,YDR360W,YKL204W,YPL018W, YPL055C,YDR448W,YKR029C,YPL182C,YER040W,YPR120C

sgf1	YFR010W,YAL013W,YGL020C,YAL021C,YGL043W,YAR002W,YAR003W,YBL058W,YGL115W,YGL127C,YGL151W,YML095C,YMR060C,YMR263W,YMR272C,YNL136W,YBR095C,YBR103W,YGL194C,YBR175W,YGL244W,YGR057C,YGR063C,YBR279W,YGR078C,YCL008C,YNL153C,YNR010W,YNR051C,YCL037C,YHL011C,YCR033W,YHL020C,YHR013C,YCR065W,YCR081W,YIL020C,YIL040W,YIR005W,YJL006C,YDL115C,YDL116W,YJL127C,YOL115W,YOR010C,YJL129C,YJL169W,YJL179W,YDR289C,YOR058C,YOR123C,YKL139W,YKL204W,YKL213C,YOR141C,YDR448W,YKR029C,YLL027W,YDR497C,YLR055C,YLR200W,YLR244C,YER083C,YPR031W,YPR057W,YPR070W,YPR120C
ubp8	YFR010W,YGL020C,YGL043W,YGL115W,YMR060C,YNL097C,YNL136W,YBR095C,YBR103W,YGL194C,YBR175W,YGL244W,YGR063C,YBR279W,YGR078C,YCL008C,YNL153C,YNR010W,YNR051C,YCL037C,YHL011C,YCR033W,YHL020C,YHR013C,YCR065W,YIL020C,YIL040W,YIL084C,YDL020C,YIR005W,YJL006C,YDL115C,YDL116W,YJL127C,YJL129C,YJL140W,YJL169W,YDR207C,YJL179W,YDR289C,YDR290W,YOR123C,YJR105W,YKL139W,YKL204W,YKL213C,YOR141C,YDR448W,YKR029C,YDR469W,YDR497C,YLR055C,YLR200W,YPL086C,YPL181W,YPL182C,YLR244C,YER083C
swr1	YFR010W,YGL043W,YBL058W,YGL115W,YGL127C,YGL151W,YNL025C,YNL136W,YBR095C,YBR175W,YBR279W,YGR078C,YCL008C,YNL153C,YNL273W,YNR010W,YNR051C,YCL037C,YHL011C,YCR033W,YHL020C,YHR013C,YHR041C,YCR077C,YIL020C,YIL040W,YDL020C,YIR005W,YDL115C,YDL116W,YJL124C,YJL127C,YOL072W,YDR159W,YJL179W,YOR026W,YOR043W,YKL213C,YPL042C,YPL055C,YDR448W,YKR029C,YDR469W,YLR015W,YLR055C,YEL061C,YER016W,YLR200W YPL182C,YLR244C,YER122C,YPR023C,YPR046W,YPR057W,YPR120C

vps72	YAL002W,YFR010W,YAL013W,YGL020C,YAL021C,YGL043W,YAR003W,YBL058W,YGL115W,YGL127C,YGL151W,YNL097C,YNL136W,YBR095C,YGR056W,YGR063C,YBR279W,YGR078C,YCL008C,YNL153C,YNR010W,YNR051C,YCL037C,YHL011C,YCR033W,YHL020C,YCR077C,YIL020C,YIL040W,YIR005W,YDL116W,YJL127C,YOL072W,YOR010C,YJL140W,YDR159W,YJL169W,YJR043C,YOR123C,YDR318W,YJR105W,YDR360W,YKL139W,YKL213C,YDR448W,YKR029C,YLL027W,YLR055C,YLR200W,YER040W,YLR244C,YPR023C,YPR031W,YPR046W,YPR057W,YPR070W,YPR120C

TABLE S4

***set3*Δ genetic interactions suppressed by the *htz1*Δ *set3*Δ suppressors**

Suppressor	Synthetic Lethal Genes Suppressed (Growth Cutoff = 1.5)
hda2	YAL013W,YBR095C,YHR167W,YIL084C,YJL168C,YLR056W,YNL097C,YPL055C
hda3	YAL013W,YBR095C,YHR167W,YJL179W,YLR056W,YNL097C,YPL055C
pre9	YAL013W,YBR095C,YBR231C,YDR334W,YER161C,YHR167W,YIL040W,YJL168C,YJL179W,YLR056W,YNL097C,YNL107W,YOL004W,YOL012C,YPL055C,YPL181W
rpn10	YHR167W,YJL179W,YLR056W,YNL097C,YNL107W,YOL004W,YPL055C
sgf11	YAL013W,YBR095C,YBR231C,YCR065W,YDR334W,YDR485C,YER161C,YHR167W,YIL084C,YJL179W,YLR056W,YLR085C,YML041C,YNL097C,YNL107W,YOL012C,YPL181W
ubp8	YAL013W,YBR095C,YBR231C,YCR065W,YDR334W,YDR485C,YER161C,YGR078C,YIL040W,YIL084C,YJL179W,YLR056W,YLR085C,YML041C,YNL097C,YNL107W,YOL004W,YOL012C,YPL055C,YPL181W